New Proposals for the Analysis and Design of Linear-Phase FBMC/OQAM Transmultiplexers

Didier Pinchon, Pierre Siohan

New Proposals for the Analysis and Design of Linear-Phase FBMC/OQAM Transmultiplexers

Didier Pinchon[1] and Pierre Siohan[2]

[1]Institut de Mathématiques, Université Paul Sabatier, Toulouse, France
[2]Independent researcher
didier.pinchon@math.univ-toulouse.fr, pierre.siohan@wanadoo.fr

March 29, 2021

Abstract

The use of filterbank formalism has now become a current practice to analyze and design MultiCarrier Modulation (MCM) systems. In this note, we reuse this powerful tool to revisit the Orthogonal Frequency Division Multiplexing (OFDM)/Offset Quadrature Amplitude Modulation(OQAM) or, equivalently, the Filter Bank MultiCarrier (FBMC)/OQAM scheme. Focusing on symmetric OFDM/OQAM systems with a number of subcarriers being a multiple of 4, we, firstly propose a complete characterization of perfect, or nearly perfect, reconstruction FBMC systems using classical tools of the linear algebra theory. In addition, we introduce two new families of prototype filters that, with a reduced number of parameters, outperform classical solutions from the literature for minimization of the total interference criterion.

1 Introduction

Introduced in the last mid-sixties the MultiCarrier Modulation (MCM) idea has become a reality along the years. Nowadays, among the various possible MCM schemes, Orthogonal Frequency Division Multiplexing (OFDM), being adopted in a large bunch of communication standards, remains, from an industrial point of view, the clear leader. Filter Bank MultiCarrier (FBMC) is another MCM option that also attracts researchers and engineers. As recalled in [1], even if it has been decided to stick to OFDM for the fifth generation (5G) mobile communications, mainly for backwards compatibility with 4G, the modulation format, and particularly the FBMC one, still needs to be investigated. Roughly speaking OFDM and FBMC systems share many commonalities, among others, it is worth mentioning the ease of implementation using fast Fourier transform algorithms and the possibility to preserve orthogonality properties in spite of the overlap between frequency subcarriers. The main difference, when considering the FBMC/Offset Quadrature Amplitude Modulation (OQAM) option, also known as OFDM/OQAM, comes from the fact that both MCM schemes do not

refer to the same type of orthogonality. If for OFDM, the orthogonality holds in the complex domain, i.e. the receiver directly attempts to recover the QAM symbols transmitted over each sub-carrier, for FBMC/OQAM the orthogonality can only be reached in the real domain, transmitting OQAM symbols, i.e. at given time and frequency locations either purely real or purely imaginary coefficients. Only satisfying a real orthogonality condition involves some additional complexity, but FBMC/OQAM has the great advantage over OFDM of allowing designers to introduce efficient filtering operations and, furthermore, can operate at a maximum transmission bit rate since no Cyclic Prefix is required.
In this note, we only focus on the FBMC/OQAM scheme corresponding to the present state of art description, i. e. the transmitted signal is generated using an exponentially modulated Synthesis Filter Bank while at the receiver side the signal is decomposed using the match filtering principle by an Analysis Filter Bank (AFB), such that the SFB-AFB pair satisfies either a perfect, or a nearly perfect, reconstruction property, being abbreviated by PR or NPR, respectively. Let us nevertheless recall a few landmarks papers that have paved the way. For interested readers, a more complete and actualized overview can be found in [2, Chapter 7]. The basic idea has been exposed at first in [3] and it originally leads to a continuous-time description of this MCM scheme often named Staggered MultiTone (SMT) either using, starting in 2010, a continuous [4] or, more recently, a discrete-time [5] description.
The OFDM/OQAM spelling came at first in reference [6] but still corresponding to a continuous-time description. A detailed description of OFDM/OQAM in discrete-time is provided in [7]. What is now called FBMC/OQAM, a denomination introduced within the European PHYDYAS project [8], globally reuses the description and implementation features introduced in [7].
In this note, our aim is to bring a new look at the FBMC/OQAM described in [7] and since then in many research papers, projects and standards. Doing so, compared to [7], we introduce one single restriction. Instead of considering FBMC/OQAM systems equipped with arbitrary length prototype filters, in the present note, we assume this length, denoted L, is expressed as $L = KM$ with K the overlapping factor and M the sub-carrier number supposed to be a multiple of 4. Note that for practical applications these conditions are generally satisfied and do not constitute veritable restrictions. For this KM-length prototype filter our aim is three-fold:

1. Revisit the link between real orthogonality and PR of the FBMC/OQAM transmultiplexer (TMUX);

2. Derive a diagonalized form of the TMUX matrix transfer function;

3. Introduce new families of NPR prototype filters.

More precisely:

- [7] provides a first proof of the equivalence between perfect real orthogonality of OFDM/OQAM systems and PR property of the associated back-to-back SFB and AFB. In the present note, we exhibit a simplified proof for KM-length FBMC systems and analyze more in details different equivalent PR conditions. In particular, we show,

for the first time with a discrete-time formalism, the link between perfect real orthogonality and the conditions that have to be satisfied by the discrete-time ambiguity function of the prototype filter.

- In various publications the transfer matrix function, say $\boldsymbol{T}$, of the FBMC/OQAM TMUX has been used to analyze its behavior, in particular w.r.t. the resulting Inter-Symbol Interference (ISI) and InterCarrier Interference (ICI). Some interesting features of $\boldsymbol{T}$ have already been mentioned, e.g. its symmetry in [7], the fact that its terms were similar in every row [9], and, more recently, its Toeplitz nature in [10]. But, up to now, no authors have taken simultaneously advantage of all these features. Doing so, in this note, we obtain a diagonalization of the transfer matrix $\boldsymbol{T}$.

- For large values of M and K, the direct computation of PR or NPR prototype filters may lead to large size difficult optimization problems. On another hand, we can notice a constant interest for the Square Root Raised Cosine (SRRC) prototype filter, that only involves one parameter, while in the case of FBMC/OQAM systems a prototype filter defined with at most K parameters, introduced independently by Martin and Mirabbasi [11, 12] and Bellanger [13], has also attracted a lot of interest, see for instance [2]. Let call MMB this prototype filter. As for the SRRC and the MMB prototype filter, our aim in this note is to propose new families of NPR prototype filters being characterized only using a limiter number of parameters. Our goal is attained starting from the Extended Gaussian Function (EGF) [14, 15, 16], a PR prototype filter if its length and number of parameters can go to infinity. A first class of NPR prototype filters is obtained using an appropriate modification of the original EGFs, named Linear Combination of Gaussian Filters (LCGF), involving at most $K + 2$ parameters. To create the second family, named GEN, we introduce another modification of the EGF. Then, with at most $2K + 3$ parameters, GEN family incorporates the LCGF and MMB families of prototype filters. All these NPR FBMC/OQAM solutions are compared taking into account an overall interference measure.

Our note is organized as follows. Section 2 is devoted to the presentation of the FBMC/OQAM prototype filter. Starting from the PR conditions involving the polyphase components of the prototype filter, sets of z-functions are introduced allowing us to derive four different PR conditions. In Section 3, we introduce a z-matrix connected to one of the previous PR condition and provide a diagonalization of this symmetric matrix. In Section 4, we rewrite the FBMC/OQAM equations corresponding to the case where $L = KM$ and, taking advantage of the linear algebra analysis introduced in Section 3, an expression of the FBMC/OQAM TMUX is derived. Then, in order to tackle the case of NPR systems, a few possible expressions for the interference functions are restated. As in [9], in Section 5, the TOtal Interference (TOI) criterion, i. e. ISI+ICI, is retained to optimize the different families of prototype filters considered in our study while usual metrics, as out-of-band energy and time-frequency localization (TFL) are used to complete our comparisons. Our conclusions are finalized in Section 6.

Notations

In this note, vectors and matrices are denoted by bold characters, and row and column indexes start from 0. j designates the imaginary unit, i. e. $j^2 = -1$. For a complex number,

say c, $\Re\{c\}$ and $\Im\{c\}$ designate its real and imaginary part, respectively. Superscript $.^T$ stands for transposition. Overlined terms denote complex conjugation, e. g. for a discrete-time filter, $p[n]$ with z-transform $P(z)$, $\overline{P(z)} = \sum_n \overline{p[n]} z^{-n}$.

For an $n \times n$ matrix $\boldsymbol{B}$ and $m \geq 2$, the $nm \times nm$ block diagonal matrix with m diagonal blocks equal to $\boldsymbol{B}$ is denoted by $\boldsymbol{D}_m[\boldsymbol{B}]$. The $n \times n$ identity matrix is denoted by $\boldsymbol{I}_n$.

If $\boldsymbol{v}$ is a vector of dimension n, $\boldsymbol{\Delta}[\boldsymbol{v}]$ is the $n \times n$ diagonal matrix such that $\boldsymbol{\Delta}[\boldsymbol{v}]_{r,r} = \boldsymbol{v}_r,\ 0 \leq r \leq n-1$.

$\boldsymbol{\Gamma}_n$ is the $n \times n$ diagonal matrix with diagonal elements $[\boldsymbol{\Gamma}_n]_{r,r} = (-1)^r,\ 0 \leq r \leq n-1$.

For $n \geq 1$, as denoted for example in [17], $\boldsymbol{C}_n^{II}$ is the $n \times n$ non normalized DCT-II matrix defined by

$$[\boldsymbol{C}_n^{II}]_{r,c} = \cos \frac{\pi r(2c+1)}{2n},\ 0 \leq r, c \leq n-1, \tag{1}$$

and $\boldsymbol{C}_n^{III}$ is the $n \times n$ non normalized DCT-III matrix defined by

$$\left[\boldsymbol{C}_n^{III}\right]_{r,c} = \begin{cases} \dfrac{1}{2} & \text{if } c = 0 \\ \cos \dfrac{(2r+1)c\pi}{2n} & \text{if } c \neq 0 \end{cases},\ 0 \leq r, c \leq n-1. \tag{2}$$

Up to a multiplicative constant, $\boldsymbol{C}_n^{II}$ and $\boldsymbol{C}_n^{III}$ are inverse matrices

$$\boldsymbol{C}_n^{II}\, \boldsymbol{C}_n^{III} = \frac{n}{2} \boldsymbol{I}_n. \tag{3}$$

Let σ be a bijective application on the set $\{0, 1, \ldots n-1\}$ for $n \geq 2$ that defines a permutation of this set. Then the $n \times n$ permutation matrix $\boldsymbol{J}_\sigma$ is defined by $[\boldsymbol{J}_\sigma]_{r,c} = 1$ if $c = \sigma(r)$ and 0 otherwise, for $0 \leq r, c \leq n-1$.
For σ and τ two permutations on $\{0, 1, \ldots n-1\}$, and $\tau \circ \sigma$ their composition defined by $\tau \circ \sigma(r) = \tau(\sigma(r)),\ 0 \leq r \leq n-1$, then $\boldsymbol{J}_\sigma\, \boldsymbol{J}_\tau = \boldsymbol{J}_{\tau \circ \sigma}$.
For a permutation σ on $\{0, 1, \ldots n-1\}$ and a vector $\boldsymbol{v}$ of dimension n,

$$\Delta[\boldsymbol{J}_\sigma \boldsymbol{v}] = \boldsymbol{J}_\sigma \Delta[\boldsymbol{v}] \boldsymbol{J}_\sigma^T. \tag{4}$$

Let s_n denote the permutation on $\{0, 1, \ldots, n-1\}$ defined by $s_n(i) = n-1-i$, and $\boldsymbol{J}_n = \boldsymbol{J}_{s_n}$ be the associated permutation matrix. The following lemma, with a straightforward proof, will be used later on.

Lemma 1. *For any $n \geq 1$, $\boldsymbol{C}_n^{III}\, \boldsymbol{\Gamma}_n = \boldsymbol{J}_n\, \boldsymbol{C}_n^{III}$.*

Proof.– For $c = 0$ and $0 \leq r \leq n-1$, we get $\left[\boldsymbol{C}_n^{III}\, \boldsymbol{\Gamma}_n\right]_{r,0} = \left[\boldsymbol{J}_n\, \boldsymbol{C}_n^{III}\right]_{r,0} = \frac{1}{2}$.
When $c \neq 0$,

$$\left[\boldsymbol{C}_n^{III}\, \boldsymbol{\Gamma}_n\right]_{r,c} \;=\; (-1)^c \cos \frac{(2r+1)c\pi}{2n},$$

$$\begin{aligned}\left[\boldsymbol{J}_n\,\boldsymbol{C}_n^{III}\right]_{r,c} &= [\boldsymbol{C}_n^{III}]_{n-1-r,c} = \cos\frac{[2(n-1-r)+1]c\pi}{2n} \\ &= \cos\left(c\pi - \frac{(2r+1)c\pi}{2n}\right) = \left[\boldsymbol{C}_n^{III}\,\boldsymbol{\Gamma}_n\right]_{r,c},\end{aligned}$$

which proves Lemma 1. □

2 FBMC/OQAM prototype filter

As indicated in the introduction, in this note we focus on M-subcarrier FBMC/OQAM systems equipped with a symmetrical prototype filter having a K overlapping factor. Beyond the brief reminder of the Perfect Reconstruction (PR) property reported in subsection 2.2, giving the condition for a distortion-free FBMC transmission, i. e. the capability to exactly recover at the demodulator output the transmitted input symbols, we introduce new functions allowing us afterwards to provide a complete and precise description of the FBMC/OQAM transmission system.

2.1 Basic definitions

For $K \geq 2$ and $M \geq 4$, M multiple of 4, we consider in this note a causal symmetric real filter $P(z) = \sum_{n=0}^{L-1} p[n]z^{-n}$ of length $L = KM$, called the *prototype filter*. So $p[n] = p[L-1-n]$ for $0 \leq n \leq L-1$.
The M-polyphase components $G_l(z),\ 0 \leq l \leq M-1$ of $P(z)$ are defined by

$$P(z) = \sum_{l=0}^{M-1} z^{-l} G_l(z^M), \tag{5}$$

and we note that $G_l(z)$ are polynomials of degree $K-1$ in z^{-1}.
If we define the functions $s(G_l)(z),\ 0 \leq l \leq M-1$, by $s(G_l)(z) = z^{-(K-1)}G_l(z^{-1})$, then the symmetry of $P(z)$ implies that $s(G_l)(z) = G_{M-1-l}(z)$ for any $0 \leq l \leq M-1$.

Let us define the functions $\lambda_r(z)$ and $b_r(z)$, $0 \leq r \leq \frac{M}{4}-1$, by

$$\lambda_r(z) = \frac{M}{2}z^{-1}\left[G_r(z)s(G_r)(z) + G_{r+\frac{M}{2}}(z)s(G_{r+\frac{M}{2}})(z)\right], \tag{6}$$

$$b_r(z) = 2(-1)^r z^{-1}\sum_{l=0}^{\frac{M}{4}-1}\left[G_r(z)s(G_r)(z) + G_{r+\frac{M}{2}}(z)s(G_{r+\frac{M}{2}})(z)\right]\cos\frac{2\pi r(2l+1)}{M}. \tag{7}$$

The $\frac{M}{4}$-vector $\boldsymbol{b}_{\frac{M}{4}}(z)$ (resp. $\boldsymbol{\lambda}_{\frac{M}{4}}(z)$) is the vector with components $b_r(z),\ \ 0 \leq r \leq \frac{M}{4}-1$ (resp. $\lambda_r(z),\ \ 0 \leq r \leq \frac{M}{4}-1$).

Let us also define two $\frac{M}{4} \times K$ matrices $\boldsymbol{V}$ and $\boldsymbol{W}$ by

$$[\boldsymbol{V}]_{r,c} = \sum_{m=0}^{2K-2c-1} p\left[r+m\frac{M}{2}\right]\ p\left[r+m\frac{M}{2}+cM\right], \tag{8}$$

$$[\boldsymbol{W}]_{r,c} \;=\; \sum_{k=0}^{L-1-cM} p[k]\, p[k+cM] \cos \frac{2\pi r(2k+1)}{M}, \tag{9}$$

for $0 \leq r \leq \frac{M}{4} - 1$, $0 \leq c \leq K-1$.

Remark 1. $[\boldsymbol{W}]_{0,0} = \|P(z)\|_2^2 = \sum_{k=0}^{L-1} p[k]^2$, *the squared* l^2*-norm of* $P(z)$.

The elements of matrix $\boldsymbol{W}$ are strongly related to the usual discrete-time ambiguity function $A_P[l,\nu]$ defined, as proposed for instance in [18], by

$$A_P[l,\nu] = e^{-j\pi\nu l} \sum_{k=0}^{L-1-l} p[k]p|k+l]e^{-j2\pi k\nu}. \tag{10}$$

Then, over a $(cM, \frac{2r}{M})$ time-frequency lattice, using the symmetry of $P(z)$, we get

$$\begin{aligned} A_P\left[cM, \frac{2r}{M}\right] &= \sum_{k=0}^{L-1-cM} p[k]p[k+cM]e^{-2j\pi k\frac{2r}{M}} \\ &= \frac{1}{2}\sum_{k=0}^{L-1-cM} p[k]p[k+cM]\left\{e^{2j\pi k\frac{2r}{M}} + e^{2j\pi(L-1-cM-k)\frac{2r}{M}}\right\}, \end{aligned} \tag{11}$$

and therefore

$$\begin{aligned} A_P\left[cM, \frac{2r}{M}\right] &= e^{-2j\pi\frac{r}{M}} \sum_{k=0}^{L-1-cM} p[k]p[k+cM] \cos \frac{2\pi r(2k+1)}{M} \\ &= e^{-2j\pi\frac{r}{M}}\,[\boldsymbol{W}]_{r,c}. \end{aligned} \tag{12}$$

Let us define the K-vector $\boldsymbol{u}(z)$ by

$$\boldsymbol{u}(z) = [z^{-K}, z^{-K+1} + z^{-K-1}, \ldots, z^{-1} + z^{-2K+1}]^T. \tag{13}$$

Proposition 1. *For* $K \geq 2$, $M \geq 4$, M *multiple of 4, and any symmetric prototype filter* $P(z)$ *of length* $L = KM$, *the following equalities are verified:*

(i) $\boldsymbol{b}_{\frac{M}{4}}(z) = \dfrac{4}{M}\,\boldsymbol{\Gamma}_{\frac{M}{4}}\,\boldsymbol{C}^{II}_{\frac{M}{4}}\,\boldsymbol{\lambda}_{\frac{M}{4}}(z)$,

(ii) $\boldsymbol{\lambda}_{\frac{M}{4}}(z) = 2\,\boldsymbol{C}^{III}_{\frac{M}{4}}\,\boldsymbol{\Gamma}_{\frac{M}{4}}\,\boldsymbol{b}_{\frac{M}{4}}(z)$,

(iii) $\boldsymbol{W} = 2\,\boldsymbol{C}^{II}_{\frac{M}{4}}\,\boldsymbol{V}$,

(iv) $\boldsymbol{\lambda}_{\frac{M}{4}}(z) = \dfrac{M}{2}\,\boldsymbol{V}\;\boldsymbol{u}(z)$,

(v) $\boldsymbol{b}_{\frac{M}{4}}(z) = \boldsymbol{\Gamma}_{\frac{M}{4}}\, \boldsymbol{W}\, \boldsymbol{u}(z)$.

Proof.– Using (6), (7), and the definitions of $\boldsymbol{\Gamma}_{\frac{M}{4}}$ and $\boldsymbol{C}^{II}_{\frac{M}{4}}$, (i) is evident.

(ii)– From (i), we get

$$\boldsymbol{\lambda}_{\frac{M}{4}}(z) = \frac{M}{4}\, \left[\boldsymbol{C}^{II}_{\frac{M}{4}}\right]^{-1}\, \boldsymbol{\Gamma}^{-1}_{\frac{M}{4}}\, \boldsymbol{b}_{\frac{M}{4}}(z).$$

As

$$\boldsymbol{\Gamma}^{-1}_{\frac{M}{4}} = \boldsymbol{\Gamma}_{\frac{M}{4}} \text{ and } \left[\boldsymbol{C}^{II}_{\frac{M}{4}}\right]^{-1} = \frac{8}{M}\, \boldsymbol{C}^{III}_{\frac{M}{4}},$$

from (3), this proves (ii).

Setting $k = a + m\frac{M}{2}$ with $0 \le a \le \frac{M}{2} - 1$, $0 \le m \le 2K - 2c - 1$ in (9) gives

$$\begin{aligned}
[\boldsymbol{W}]_{r,c} &= \sum_{a=0}^{\frac{M}{2}-1} \sum_{m=0}^{2K-2c-1} p\left[a + m\frac{M}{2}\right] p\left[a + m\frac{M}{2} + cM\right] \cos\frac{2\pi r(2a+1)}{M} \\
&= \sum_{a=0}^{\frac{M}{4}-1} \sum_{m=0}^{2K-2c-1} p\left[a + m\frac{M}{2}\right] p\left[a + m\frac{M}{2} + cM\right] \cos\frac{2\pi r(2a+1)}{M} + \\
&\quad \sum_{a=\frac{M}{4}}^{\frac{M}{2}-1} \sum_{m=0}^{2K-2c-1} p\left[a + m\frac{M}{2}\right] p\left[a + m\frac{M}{2} + cM\right] \cos\frac{2\pi r(2a+1)}{M}.
\end{aligned}$$

In the second sum, we set $a = \frac{M}{2} - 1 - b$ and $m = 2K - 2c - 1 - m'$ and using the cosine equality $\cos\frac{2\pi r(2a+1)}{M} = \cos\frac{2\pi r(2b+1)}{M}$, we find that

$$\begin{aligned}
p\left[a + m\frac{M}{2}\right] &= p\left[KM - 1 - (b + m'\frac{M}{2} + cM)\right] = p\left[b + m'\frac{M}{2} + cM\right], \\
p\left[a + m\frac{M}{2} + cM\right] &= p\left[KM - 1 - (b + m'\frac{M}{2})\right] = p\left[b + m'\frac{M}{2}\right],
\end{aligned}$$

Then, using the symmetry of $P(z)$, we get

$$\begin{aligned}
[\boldsymbol{W}]_{r,c} &= 2\sum_{a=0}^{\frac{M}{4}-1} \cos\frac{2\pi r(2a+1)}{M} \sum_{m=0}^{2K-2c-1} p\left[a + m\frac{M}{2}\right] p\left[a + m\frac{M}{2} + cM\right] \\
&= 2\sum_{a=0}^{\frac{M}{4}-1} \left[\boldsymbol{C}^{II}_{\frac{M}{4}}\right]_{r,a} [\boldsymbol{V}]_{a,c} \ ,
\end{aligned}$$

which proves (iii).

(iv) is equivalent to

$$\lambda_r(z) = \frac{M}{2} \sum_{k=1}^{2K-1} [\boldsymbol{V}]_{r,|K-k|}\, z^{-k},\ 0 \le r \le \frac{M}{4} - 1. \tag{14}$$

For $0 \leq r \leq \frac{M}{4} - 1$, $R_r(z) = G_r(z)s(G_r)(z) + G_{r+\frac{M}{2}}(z)s(G_{r+\frac{M}{2}})(z)$ is a polynomial of degree $2K-2$ in z^{-1}, satisfying $z^{-(2K-2)}R_r(z^{-1}) = R_r(z)$, that can therefore be written as

$$R_r(z) = c_{r,0}z^{-(K-1)} + \sum_{k=1}^{K-1} c_{r,k}\left(z^{-(K-1-k)} + z^{-(K-1+k)}\right), \tag{15}$$

with coefficients $c_{r,k}$, $0 \leq k \leq K-1$. Rewriting the polyphase components and using $P(z)$ symmetry, we get

$$\begin{aligned} G_r(z) &= \sum_{n=0}^{K-1} p[r+nM]\, z^{-n}, \\ s(G_r(z)) &= G_{M-1-r}(z) = \sum_{m=0}^{K-1} p[M-1-r+mM]\, z^{-m} \\ &= \sum_{m=0}^{K-1} p[(K-1-m)M+r]\, z^{-m}, \end{aligned}$$

The coefficient $d_{r,k}^{(1)}$ of $z^{-(K-1-k)}$ in $G_r(z)s(G_r)(z)$ is obtained by keeping the term in the product such that $n+m = K-1-k$, i.e. $m = K-1-k-n$ and $0 \leq n \leq K-1-k$, and therefore

$$\begin{aligned} d_{r,k}^{(1)} &= \sum_{n=0}^{K-1-k} p[r+nM]\, p[r+nM+kM] \\ &= \sum_{n=0}^{K-1-k} p\left[r+2n\frac{M}{2}\right]\, p\left[r+2n\frac{M}{2}+kM\right] \end{aligned}$$

In the same way, we get that the coefficient $d_{r,k}^{(2)}$ of $z^{-(K-1-k)}$ in $G_{r+\frac{M}{2}}(z)s(G_{r+\frac{M}{2}})(z)$ is

$$d_{r,k}^{(2)} = \sum_{n=0}^{K-1-k} p\left[r+(2n+1)\frac{M}{2}\right]\, p\left[r+(2n+1)\frac{M}{2}+kM\right],$$

and since $c_{r,k} = d_{r,k}^{(1)} + d_{r,k}^{(2)}$, using the definition (8), it comes that

$$\begin{aligned} c_{r,k} &= \sum_{n=0}^{2K-2k-1} p\left[r+n\frac{M}{2}\right]\, p\left[r+n\frac{M}{2}+kM\right] \\ &= [\boldsymbol{V}]_{r,k}, \end{aligned} \tag{16}$$

This proves (iv).

From (i), (iv) and (iii), we get

$$\boldsymbol{b}_{\frac{M}{4}}(z) = 2\,\boldsymbol{\Gamma}_{\frac{M}{4}}\,\boldsymbol{C}_{\frac{M}{4}}^{II}\,\boldsymbol{V}\,\boldsymbol{u}(z)$$

$$= \quad \mathbf{\Gamma}_{\frac{M}{4}}\, \boldsymbol{W}\, \boldsymbol{u}(z), \tag{17}$$

which is (v).
In an equivalent way, (v) may be written

$$b_r(z) = (-1)^r \sum_{k=1}^{2K-1} [\boldsymbol{W}]_{r,|K-k|}\; z^{-k},\; 0 \leq r \leq \frac{M}{4} - 1. \tag{18}$$

□

2.2 Perfect reconstruction property

Directly deduced from [7], we can say that a FBMC/OQAM symmetric prototype filter $P(z)$ of length $L = KM$ with $K \geq 2$ and $M \geq 4$, M multiple of 4, is PR if its M-polyphase components $G_l(z)$ satisfy the equalities

$$G_l(z)s(G_l)(z) + G_{l+\frac{M}{2}}(z)s(G_{l+\frac{M}{2}})(z) = \frac{2\alpha}{M}\, z^{-K+1},\; 0 \leq l \leq \frac{M}{4} - 1, \tag{19}$$

where $\alpha = \|P(z)\|_2^2$.

Proposition 2. *The PR property of such a symmetric filter $P(z)$ is equivalent to any of the following assertions:*

(i) $b_0(z) = \alpha z^{-K}$ *and* $b_r(z) = 0,\; 1 \leq r \leq \frac{M}{4} - 1,$

(ii) $\lambda_r(z) = \alpha z^{-K},\; 0 \leq r \leq \frac{M}{4} - 1,$

(iii) $\boldsymbol{V}$ *verifies* $[\boldsymbol{V}]_{r,c} = \frac{2\alpha}{M}$ *if* $c = 0$, *and* 0 *otherwise,*

(iv) $\boldsymbol{W}$ *verifies* $[\boldsymbol{W}]_{0,0} = \alpha$ *and* $[\boldsymbol{W}]_{r,c} = 0$ *if* $(r,c) \neq (0,0)$.

Proof.– Using the definition of $b_r(z)$ by equation (7) and (19) gives immediately (ii). From equation (18), that expresses the coefficients in z^{-1} as elements of matrix $\boldsymbol{W}$, we get (iv).

From Proposition 1 (iii) and then by (3) we obtain

$$\boldsymbol{V} = \quad \tfrac{1}{2} \left[\boldsymbol{C}^{II}_{\frac{M}{4}}\right]^{-1} \boldsymbol{W} = \tfrac{4}{M}\, \boldsymbol{C}^{III}_{\frac{M}{4}}\, \boldsymbol{W},$$

and (iii) is therefore a direct consequence of (iv). Note also that (iii) equivalent to the PR condition derived in [19] for cosine modulated filter banks.
As the coefficients of matrix $\boldsymbol{V}$ are related to coefficients of functions $\lambda_r(z),\; 0 \leq r \leq \frac{M}{4} - 1$, by equation (14), (ii) is obtained. □

3 Diagonalization of a special symmetric matrix

One key element to get a precise overview of the FBMC/OQAM transmultiplexer (TMUX) is provided with its transfer matrix expression. As shown in [7, (38)], this $M \times M - \boldsymbol{T}$ matrix involves an alternation of zeros and non-zeros terms along its rows and columns. All these systematic zeros are a direct consequence, for the FBMC/OQAM scheme, of the alternate transmission in time and frequency of purely real and purely imaginary symbols. In [7] and later on also in [9, 20] this matrix has been efficiently used to derive interference expressions permitting useful comparisons between different prototype filters.
As already noted, the $\boldsymbol{T}$ matrix possesses interesting properties, symmetry [7, page 1176], similarity in every row [9] and a Toeplitz structure [10]. Exploiting all these features, in this section, we propose a self-contained analysis with its main theorem, number 2, leading to a simple diagonalization allowing us to provide afterwards a simplified FBMC/OQAM presentation.
Let n be an even positive integer and $\frac{n}{2}$ parameters $b_r,\ 0 \leq r \leq \frac{n}{2}-1$ defining the $\frac{n}{2}$ vector $\boldsymbol{b}_{\frac{n}{2}} = [b_0, b_1, \ldots, b_{\frac{n}{2}-1}]^T$.

The $n \times n$ symmetric matrix $\boldsymbol{B}_n$ is defined, for $0 \leq i, j \leq n-1$, by

$$[\boldsymbol{B}_n]_{i,j} = \begin{cases} b_r & \text{if } |i-j| = r < \frac{n}{2}, \\ -b_{n-r} & \text{if } |i-j| = r > \frac{n}{2}, \\ 0 & \text{otherwise.} \end{cases} \tag{20}$$

$\boldsymbol{B}_n$ is a special case of a symmetric Toeplitz matrix, [21, section 4.7], considered in the literature as a kind of structured matrices for which fast computation algorithms have been developed (see e.g. [22]), [23]).

In this section, a complete characterization of the spectral properties of $\boldsymbol{B}_n$ is given in Theorem 2 but first the following special case is studied where $b_0 = 0,\ b_1 = 1,\ b_r = 0,\ 2 \leq r \leq \frac{n}{2}-1$. A special name $\boldsymbol{U}_n$ is reserved for this matrix. For example, when $n = 6$,

$$\boldsymbol{U}_6 = \begin{bmatrix} 0 & 1 & 0 & 0 & 0 & -1 \\ 1 & 0 & 1 & 0 & 0 & 0 \\ 0 & 1 & 0 & 1 & 0 & 0 \\ 0 & 0 & 1 & 0 & 1 & 0 \\ 0 & 0 & 0 & 1 & 0 & 1 \\ -1 & 0 & 0 & 0 & 1 & 0 \end{bmatrix}. \tag{21}$$

Theorem 1. *The eigenvalues of $\boldsymbol{U}_n$ are $\nu_c = 2\cos\frac{(4c+1)\pi}{n},\ 0 \leq c \leq \frac{n}{2}-1$, each of them with multiplicity 2.*
We denote by $\boldsymbol{\nu}$ the $\frac{n}{2}$ vector $\boldsymbol{\nu} = [\nu_0, \nu_1, \ldots, \nu_{\frac{n}{2}-1}]^T$ and by $\boldsymbol{\Delta}_{\frac{n}{2}}(\boldsymbol{\nu})$ the diagonal $\frac{n}{2} \times \frac{n}{2}$ matrix with diagonal elements $\nu_c,\ 0 \leq c \leq \frac{n}{2}-1$.
The $n \times n$ matrix $\boldsymbol{R}_n$ defined by

$$[\boldsymbol{R}_n]_{r,c} = \frac{\sqrt{2}}{\sqrt{n}} \cos\frac{(r+c+4rc)\pi}{n},\ 0 \leq r, c \leq n-1, \tag{22}$$

is a symmetric orthogonal matrix and

$$\boldsymbol{R}_n \boldsymbol{U}_n \boldsymbol{R}_n = \boldsymbol{D}_2[\boldsymbol{\Delta}_{\frac{n}{2}}(\boldsymbol{\nu})]. \tag{23}$$

Proof.– For $0 \leq c \leq n-1$, let us denote by $\boldsymbol{V}_c$ the column of index c of $\boldsymbol{R}_n$. We get

$$\begin{aligned} ||\boldsymbol{V}_c||^2 &= \frac{2}{n}\sum_{r=0}^{n-1} \cos^2 \frac{(r+c+4rc)\pi}{n} \\ &= \frac{2}{n}\sum_{r=0}^{n-1} \frac{1}{2}\left[1+\cos\frac{2(r+c+4rc)\pi}{n}\right] \\ &= 1+\frac{1}{n}\Re\left[e^{\frac{j2\pi c}{n}}\sum_{r=0}^{n-1} e^{\frac{2j\pi(1+4c)r}{n}}\right] \\ &= 1, \end{aligned}$$

the last sum, estimated as the sum of a geometric sequence, being null.

Using usual trigonometric formulas, it is straightforward to verify that, for $0 \leq c \leq \frac{n}{2}-1$, $\boldsymbol{U}_n\boldsymbol{V}_c = \nu_c \boldsymbol{V}_c$ and $\boldsymbol{U}_n\boldsymbol{V}_{c+\frac{n}{2}} = \nu_c \boldsymbol{V}_{c+\frac{n}{2}}$, that is $\boldsymbol{V}_c$ and $\boldsymbol{V}_{c+\frac{n}{2}}$ are eigenvectors of $\boldsymbol{U}_n$ for eigenvalue ν_c.

Because eigenspaces of a real symmetric matrix for different eigenvalues are orthogonal, it remains to show that $\boldsymbol{V}_c$ and $\boldsymbol{V}_{c+\frac{n}{2}}$ are orthogonal $0 \leq c \leq \frac{n}{2}-1$. This is easily done using trigonometric formulas:

$$\begin{aligned} \boldsymbol{V}_c.\boldsymbol{V}_{c+\frac{n}{2}} &= \frac{2}{n}\sum_{r=0}^{n-1} \cos\left(\frac{(r+c+4rc)\pi}{n}\right)\cos\left(\frac{(r+c+\frac{n}{2}+4r(c+\frac{n}{2})\pi}{n}\right) \\ &= \frac{1}{n}\sum_{r=0}^{n-1}\left\{\cos\left(\frac{2(r+c+4rc)\pi}{n}+\frac{\pi}{2}+2\pi r\right)+\cos\left(\frac{\pi}{2}+2\pi r\right)\right\} \\ &= -\frac{1}{n}\Im\left[e^{\frac{j2\pi c}{n}}\sum_{r=0}^{n-1} e^{\frac{2j\pi(1+4c)r}{n}}\right] \\ &= 0. \end{aligned}$$

□

Remark 2. *Because $\boldsymbol{R}_n$ is symmetric, $\boldsymbol{R}_n^2 = \boldsymbol{I}_n$.*
The eigenvalues of $\boldsymbol{R}_n$ are $+1$ and -1, each of them with multiplicity $\frac{n}{2}$, with respective eigenspaces E_{+1} and E_{-1}. $\boldsymbol{R}_n$ is the matrix of the orthogonal symmetry in $\mathbb{R}^n$ with respect to E_{+1} (parallel to E_{-1}).

Let us consider now the $n \times n$ matrices, $\boldsymbol{U}_n^{(c)}$, $0 \leq c \leq \frac{n}{2}-1$, defined by, for $0 \leq i,j \leq n-1$,

$$[\boldsymbol{U}_n^{(c)}]_{i,j} = \begin{cases} 1 & \text{if } |i-j| = c, \\ -1 & \text{if } |i-j| = n-c, \\ 0 & \text{otherwise.} \end{cases} \tag{24}$$

It immediately comes that $\boldsymbol{U}_n^{(0)} = \boldsymbol{I}_n$, $\boldsymbol{U}_n^{(1)} = \boldsymbol{U}_n$ and

$$\boldsymbol{B}_n = \sum_{c=0}^{\frac{n}{2}-1} b_c \, \boldsymbol{U}_n^{(c)}. \tag{25}$$

Proposition 3. *The matrices $\boldsymbol{U}_n^{(c)}$ may be expressed as polynomials of $\boldsymbol{U}_n$ as follows:*

$$\boldsymbol{U}_n^{(c)} = 2T_c\left(\frac{1}{2}\boldsymbol{U}_n\right),\ 1 \le c \le \frac{n}{2} - 1, \tag{26}$$

where T_c is the first kind Chebyshev polynomial of degree c ($T_c(\cos\theta) = \cos c\theta$).

From (25) and Proposition 3, it follows that $\boldsymbol{B}_n$ may be expressed as a polynomial function of $\boldsymbol{U_n}$ as

$$\boldsymbol{B}_n = b_0\boldsymbol{I}_n + 2\sum_{c=1}^{\frac{n}{2}-1} b_c \, T_c\left(\frac{1}{2}\boldsymbol{U}_n\right). \tag{27}$$

Theorem 2. *The eigenvalues of $\boldsymbol{B}_n$ are the numbers*

$$\mu_r = b_0 + 2\sum_{c=0}^{\frac{n}{2}-1} b_c \cos\frac{(4r+1)c\pi}{n},\ 0 \le r \le \frac{n}{2} - 1, \tag{28}$$

each of them with multiplicity 2.
If we denote by $\boldsymbol{\mu}$ the $\frac{n}{2}$ vector $\boldsymbol{\mu} = [\mu_0, \mu_1, \ldots, \mu_{\frac{n}{2}-1}]^T$ and by $\boldsymbol{\Delta}_{\frac{n}{2}}(\boldsymbol{\mu})$ the diagonal $\frac{n}{2} \times \frac{n}{2}$ matrix with diagonal elements μ_c, $0 \le c \le \frac{n}{2} - 1$,

$$\boldsymbol{R}_n\boldsymbol{B}_n\boldsymbol{R}_n = \boldsymbol{D}_2[\boldsymbol{\Delta}_{\frac{n}{2}}(\boldsymbol{\mu})]. \tag{29}$$

Proof.– Using equation (27), the eigenvalues of $\boldsymbol{B}_n$ are the numbers

$$\mu_r = b_0 + 2\sum_{c=1}^{\frac{n}{2}-1} b_c \, T_c(\frac{1}{2}\nu_r),\ 0 \le r \le \frac{n}{2} - 1, \tag{30}$$

with multiplicity 2. Because

$$T_c(\frac{1}{2}\nu_r) = T_c(\cos\frac{(4r+1)\pi}{n}) = \cos\frac{(4r+1)c\pi}{n}, \tag{31}$$

we get (28).
With the same change of basis $\boldsymbol{R}_n$ than for $\boldsymbol{U}_n$, using (23), we therefore obtain the diagonalization relation (29). □

Example 1. *For $n = 6$,*

$$\boldsymbol{B}_6 = \begin{bmatrix} b_0 & b_1 & b_2 & 0 & -b_2 & -b_1 \\ b_1 & b_0 & b_1 & b_2 & 0 & -b_2 \\ b_2 & b_1 & b_0 & b_1 & b_2 & 0 \\ 0 & b_2 & b_1 & b_0 & b_1 & b_2 \\ -b_2 & 0 & b_2 & b_1 & b_0 & b_1 \\ -b_1 & -b_2 & 0 & b_2 & b_1 & b_0 \end{bmatrix}, \tag{32}$$

$$\boldsymbol{R}_6 = \frac{\sqrt{3}}{3}\begin{bmatrix} 1 & \frac{\sqrt{3}}{2} & \frac{1}{2} & 0 & -\frac{1}{2} & -\frac{\sqrt{3}}{2} \\ \frac{\sqrt{3}}{2} & -1 & \frac{\sqrt{3}}{2} & -\frac{1}{2} & 0 & \frac{1}{2} \\ \frac{1}{2} & \frac{\sqrt{3}}{2} & -\frac{1}{2} & -\frac{\sqrt{3}}{2} & \frac{1}{2} & \frac{\sqrt{3}}{2} \\ 0 & -\frac{1}{2} & -\frac{\sqrt{3}}{2} & -1 & -\frac{\sqrt{3}}{2} & -\frac{1}{2} \\ -\frac{1}{2} & 0 & \frac{1}{2} & -\frac{\sqrt{3}}{2} & 1 & -\frac{\sqrt{3}}{2} \\ -\frac{\sqrt{3}}{2} & \frac{1}{2} & \frac{\sqrt{3}}{2} & -\frac{1}{2} & -\frac{\sqrt{3}}{2} & \frac{1}{2} \end{bmatrix}. \tag{33}$$

$$\boldsymbol{D}_2[\boldsymbol{\Delta}_3(\boldsymbol{\mu})] = \begin{bmatrix} \mu_0 & 0 & 0 & 0 & 0 & 0 \\ 0 & \mu_1 & 0 & 0 & 0 & 0 \\ 0 & 0 & \mu_2 & 0 & 0 & 0 \\ 0 & 0 & 0 & \mu_0 & 0 & 0 \\ 0 & 0 & 0 & 0 & \mu_1 & 0 \\ 0 & 0 & 0 & 0 & 0 & \mu_2 \end{bmatrix}, \tag{34}$$

with

$$\mu_0 = b_0 + \sqrt{3}\, b_1 + b_2,\ \mu_1 = b_0 - \sqrt{3}\, b_1 + b_2,\ \mu_2 = b_0 - 2\, b_2. \tag{35}$$

Remark 3. *Equations (28) may be expressed by the following matrix equality*

$$\boldsymbol{\mu}_{\frac{n}{2}} = \boldsymbol{C}_{\frac{n}{2}}\ \boldsymbol{b}_{\frac{n}{2}} \tag{36}$$

where $\boldsymbol{C}_{\frac{n}{2}}$ *is the* $\frac{n}{2} \times \frac{n}{2}$ *matrix defined by*

$$\left[\boldsymbol{C}_{\frac{n}{2}}\right]_{r,c} = \begin{cases} 1 & \text{if } c = 0 \\ 2\cos\frac{(4r+1)c\pi}{n} & \text{if } c \neq 0 \end{cases},\ 0 \leq r, c \leq \frac{n}{2} - 1. \tag{37}$$

Considering the permutation $\tau = [\tau_0, \tau_1, \ldots, \tau_{\frac{n}{2}-1}]$ *of* $\{0, 1, \ldots, \frac{n}{2} - 1\}$ *obtained by the list of even indexes in* $\{0, 1, \ldots, \frac{n}{2} - 1\}$ *in increasing order followed by the list of odd indexes in decreasing order,* $\boldsymbol{J}_\tau$ *is the permutation matrix associated to* τ*, and the following relation is verified*

$$\boldsymbol{C}_{\frac{n}{2}} = 2\boldsymbol{J}_\tau\, \boldsymbol{C}^{III}_{\frac{n}{2}}. \tag{38}$$

Remark 4. *Theorem 2 is an evidence for* $n = 2$*, since* $\mu_0 = b_0$*,* $\boldsymbol{b}_1 = \boldsymbol{\mu}_1 = [\mu_0]$*,* $\boldsymbol{R}_2 = \boldsymbol{I}_2$*, and* $\boldsymbol{B}_2 = \mu_0 \boldsymbol{I}_2 = \boldsymbol{D}_2[\boldsymbol{\mu}_0]$*.*

4 The FBMC/OQAM transmultiplexer

4.1 Structure of the TMUX transfer matrix

The FBMC/OQAM transmultiplexer corresponds to the direct concatenation of the Synthesis Filter Bank (SFB), at the transmitter side, and of the Analysis Filter Bank (AFB) at the receiver side. In this note, we consider the basic TMUX system represented in Figure 1, for given $K \geq 2$ and even $M \geq 4$ multiple of 4.

It is a simple variant of a well-known scheme presented at first in [7, Figure 1] and later on in [20, Figure 2.1]. Indeed in Figure 1, without loss of generality, we only focus on the transmission of the real data symbols, say the $a_{m,n}$, with z-transform expressed as $X_m(z) =$

$\sum_n a_{m,n} z^{-n}$, thus omitting the complex-to-real conversion at the transmission side and the dual operation at the receiver side.
For given values of K and M, $P(z)$ is a symmetric prototype filter such as defined in section 2 and the synthesis and analysis filters $F_m(z),\ 0 \leq m \leq M-1$, are derived from $P(z)$ by $F_m(z) = \sum_{n=0}^{L-1} f_m[n] z^{-n}$ with

$$f_m[n] = p[n] e^{\frac{2j\pi m}{M}(n-\frac{L-1}{2})},\ 0 \leq n \leq L-1. \tag{39}$$

It comes that $F_0(z) = P(z),\ F_{M-m}(z) = -\overline{F_m(z)},\ 1 \leq m \leq M-1$, where $\overline{F_m(z)} = \sum_{n=0}^{L-1} \overline{f_m[n]} z^{-n}$.
The $F_m(z)$ are linear phase filters, i.e.

$$f_m[L-1-n] = \overline{f_m[n]},\ 0 \leq n \leq L-1,\ 0 \leq m \leq M-1. \tag{40}$$

We get

$$F_m(z) \ = \ \sum_{n=0}^{L-1} p[n] e^{\frac{2j\pi m}{M}(n-\frac{L-1}{2})} z^{-n} = e^{-\frac{j\pi m(L-1)}{M}} P\left(e^{-\frac{2j\pi m}{M}} z\right), \tag{41}$$

and, from (5),

$$F_m(z) = e^{-\frac{j\pi m(L-1)}{M}} \sum_{l=0}^{M-1} e^{\frac{2j\pi ml}{M}} G_l(z^M) z^{-l}. \tag{42}$$

In Figure 1, the multiplicative operators act as shown below

$$U(z) \rightarrow \otimes \rightarrow V(z) = j^m\, U(-jz). \qquad \uparrow\, j^{n+m} \tag{43}$$

and

$$U(z) \rightarrow \otimes \rightarrow V(z) = j^{-m}\, U(jz). \qquad \uparrow\, j^{-(n+m)} \tag{44}$$

The $\frac{M}{2}$ upsampling and downsampling operators are denoted by $\mathcal{U}_{\frac{M}{2}}$ and $\mathcal{D}_{\frac{M}{2}}$, respectively.
$X_m(z)$ and $\hat{X}_m(z)$, $0 \leq m \leq M-1$ are z-transforms of real data sequences and we denote by $\boldsymbol{X}(z)$ (resp. $\hat{\boldsymbol{X}}(z)$) the M-vector $\boldsymbol{X}(z) = [X_0(z), X_1(z), \ldots, X_{M-1}]^T$ (resp. $\hat{\boldsymbol{X}}(z) = [\hat{X}_0(z), \hat{X}_1(z), \ldots, \hat{X}_{M-1}(z)]^T$).

Let us define the $M \times M$ permutation matrix $\boldsymbol{J}_\sigma$, where σ is the permutation defined on $\{0, 1, \ldots, M-1\}$, by

$$\sigma(2r) = r,\ \sigma(2r+1) = \frac{M}{2} + r,\ 0 \leq r \leq \frac{M}{2} - 1, \tag{45}$$

and the $\frac{M}{4} \times \frac{M}{4}$ permutation matrix $\boldsymbol{J}_{\bar{\tau}}$ where $\bar{\tau}$ is the permutation defined on $\{0, 1, \ldots, \frac{M}{4}-1\}$ by

$$\bar{\tau}(i) = \begin{cases} \frac{M}{4} - 1 - 2i, & 0 \leq i \leq \lfloor \frac{M-4}{8} \rfloor, \\ 2i - \frac{M}{4}, & \lfloor \frac{M+4}{8} \rfloor \leq i \leq \frac{M}{4} - 1. \end{cases} \tag{46}$$

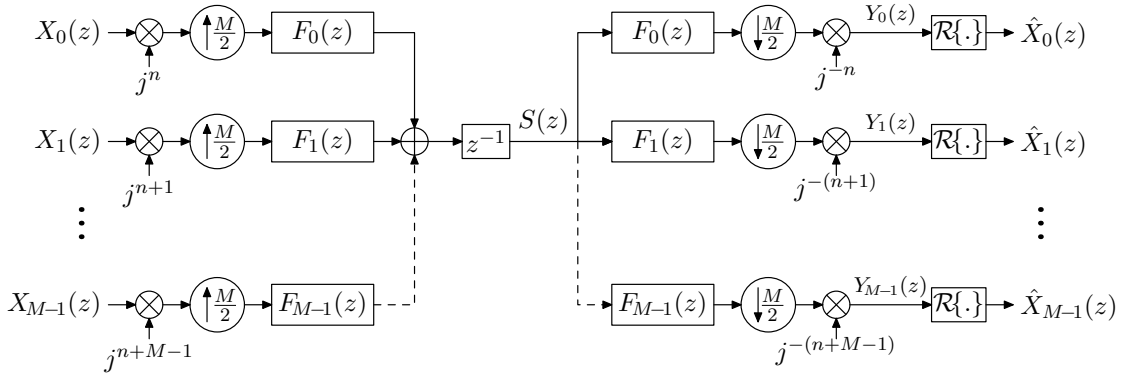

Figure 1: The basic FBMC/OQAM TMUX system for linear-phase synthesis and analysis filter banks.

Theorem 3. *For $K \geq 3$, $M \geq 4$ a multiple of 4 and $P(z)$ a symmetric real prototype filter $P(z)$ of length $L = KM$, using the definitions of section 2, the following properties are verified.*

(i) The $M \times M$ transfer matrix $\boldsymbol{T}(z)$ of the TMUX represented in Figure 1, i.e. $\hat{\boldsymbol{X}}(z) = \boldsymbol{T}(z)\,\boldsymbol{X}(z)$, is symmetric and satisfies, for $0 \leq i, j \leq M-1$,

$$[\boldsymbol{T}]_{i,j}(z) = \begin{cases} b_r(-z^2) & \text{if } |i-j| = 2r,\ 0 \leq r < \frac{M}{4}, \\ -b_r(-z^2) & \text{if } |i-j| = M-2r,\ 0 \leq r < \frac{M}{4}, \\ 0 & \text{otherwise.} \end{cases} \tag{47}$$

(ii) The eigenvalues of $\boldsymbol{T}(z)$ are the numbers $\lambda_r(-z^2)$, $0 \leq r \leq \frac{M}{4} - 1$, distinct or not, each of them with multiplicity 4.

(iii) The following matrix equality is verified

$$\boldsymbol{T}(z) = \boldsymbol{U}\,\boldsymbol{D}_4[\boldsymbol{\Delta}(\boldsymbol{\lambda}_{\frac{M}{4}}(-z^2))]\,\boldsymbol{U}^T, \tag{48}$$

where $\boldsymbol{U}$ is the constant (not depending on z^{-1}) $M \times M$ orthogonal matrix

$$\boldsymbol{U} = \boldsymbol{J}_\sigma\,\boldsymbol{D}_2[\boldsymbol{R}_{\frac{M}{2}}]\,\boldsymbol{D}_4[\boldsymbol{J}_{\bar{\tau}}], \tag{49}$$

and $\boldsymbol{R}_{\frac{M}{2}}$ is defined in section 3.

(iv) The output signals $\hat{\boldsymbol{X}}(z)$ are proportional to a delayed copy of the input signals $\boldsymbol{X}(z)$ if and only if $P(z)$ has the perfect reconstruction property. In this case $\hat{\boldsymbol{X}}(z) = (-1)^K \alpha z^{-2K} \boldsymbol{X}(z)$ with $\alpha = \|P(z)\|_2^2$.

Proof.– (i) – First remark that the application $f : \boldsymbol{X}(z) \to \hat{\boldsymbol{X}}(z)$ is linear. For $0 \leq m \leq M-1$, let us consider the vector $\boldsymbol{X}_m(z) = [X_0(z), X_1(z), \ldots, X_{M-1}]^T$ with $X_{m'}(z) = 0$, $0 \leq m' \leq M-1$, $m' \neq m$ and $X_m(z) = 1$.

Because, $f(z^{-n}\boldsymbol{X}_m(z)) = z^{-n}f(\boldsymbol{X}_m(z))$, it is sufficient to prove (i) for input signals $\boldsymbol{X}_m(z),\ 0 \leq m \leq M-1$.

For input signals $\boldsymbol{X}_m(z)$, we get

$$S(z) \;=\; j^m z^{-1} F_m(z), \tag{50}$$

and, using (42), for any $0 \leq m' \leq M-1$,

$$\begin{aligned} S(z)F_{m'}(z) &= j^m z^{-1} e^{-\frac{j\pi(m+m')(L-1)}{M}} \left[\sum_{l=0}^{M-1} e^{\frac{2j\pi ml}{M}} G_l(z^M) z^{-l}\right]\left[\sum_{l'=0}^{M-1} e^{\frac{2j\pi m'l'}{M}} G_{l'}(z^M) z^{-l'}\right] \\ &= j^m e^{-\frac{j\pi(m+m')(L-1)}{M}} \sum_{l,l'=0}^{M-1} e^{\frac{2j\pi(ml+m'l')}{M}} G_l(z^M) G_{l'}(z^M) z^{-(l+l'+1)}. \end{aligned} \tag{51}$$

Because $1 \leq l+l'+1 \leq 2M-1$, powers of $z^{\frac{M}{2}}$ appear in (51) only if $l+l'+1 = \frac{M}{2}$, $l+l'+1 = M$ and $l+l'+1 = \frac{3M}{2}$, and

$$\mathcal{D}_{\frac{M}{2}}\left[S(z)F_{m'}(z)\right] \;=\; T_1(z) + T_2(z) + T_3(z), \tag{52}$$

with

$$T_1(z) \;=\; j^m (-1)^{m'} e^{-\frac{j\pi(m+m')L}{M}} e^{\frac{j\pi(m-m')}{M}} z^{-1} \sum_{l=0}^{\frac{M}{2}-1} e^{\frac{2j\pi(m-m')l}{M}} G_l(z^2) G_{\frac{M}{2}-1-l}(z^2), \tag{53}$$

$$T_2(z) \;=\; j^m e^{-\frac{j\pi(m+m')L}{M}} e^{\frac{j\pi(m-m')}{M}} z^{-2} \sum_{l=0}^{M-1} e^{\frac{2j\pi(m-m')l}{M}} G_l(z^2) G_{M-1-l}(z^2), \tag{54}$$

$$T_3(z) \;=\; j^m (-1)^{m'} e^{-\frac{j\pi(m+m')L}{M}} e^{\frac{j\pi(m-m')}{M}} z^{-3} \sum_{l=\frac{M}{2}}^{M-1} e^{\frac{2j\pi(m-m')l}{M}} G_l(z^2) G_{\frac{3M}{2}-1-l}(z^2). \tag{55}$$

From (53), we get

$$\begin{aligned} j^{-m'} T_1(jz) &= (-1)^{m'} j^{m-m'+1} e^{-\frac{j\pi(m+m')L}{M}} e^{\frac{j\pi(m-m')}{M}} z^{-1} \sum_{l=0}^{\frac{M}{2}-1} e^{\frac{2j\pi(m-m')l}{M}} G_l(-z^2) G_{\frac{M}{2}-1-l}(-z^2), \\ &= (-1)^{m'} j^{m-m'+1} e^{-\frac{j\pi(m+m')L}{M}} e^{\frac{j\pi(m-m')}{M}} \times \\ &\quad z^{-1} \sum_{l=0}^{\frac{M}{4}-1} \left[e^{\frac{2j\pi(m-m')l}{M}} + e^{\frac{2j\pi(m-m')(\frac{M}{2}-1-l)}{M}}\right] G_l(-z^2) G_{\frac{M}{2}-1-l}(-z^2), \\ &= 2(-1)^{m'} j^{m-m'+1} e^{-\frac{j\pi(m+m')L)}{M}} e^{\frac{j\pi(m-m')}{2}} \times \\ &\quad z^{-1} \sum_{l=0}^{\frac{M}{4}-1} G_l(-z^2) G_{\frac{M}{2}-1-l}(-z^2) \cos\frac{\pi(m-m')(4l+2-M)}{2M}, \end{aligned} \tag{56}$$

and therefore, after simplification,

$$j^{-m'}T_1(jz) = 2j(-1)^{(m+m')K+m}z^{-1}\sum_{l=0}^{\frac{M}{4}-1} G_l(-z^2)G_{\frac{M}{2}-1-l}(-z^2)\cos\frac{\pi(m-m')(4l+2-M)}{2M},$$

and

$$\mathcal{R}\{j^{-m'}T_1(jz)\} = 0,\ 0 \le m, m' \le M-1. \tag{57}$$

In the same way, using (55), it is proved that

$$\mathcal{R}\{j^{-m'}T_3(jz)\} = 0,\ 0 \le m, m' \le M-1. \tag{58}$$

From (54), we get

$$\begin{aligned} j^{-m'}T_2(jz) &= j^{m-m'+2}e^{-\frac{j\pi(m+m')L}{M}}e^{\frac{j\pi(m-m')}{M}}z^{-2}\sum_{l=0}^{M-1} e^{\frac{2j\pi(m-m')l}{M}}G_l(-z^2)G_{M-1-l}(-z^2), \\ &= (-1)^{(m+m')K}j^{m-m'+2}e^{\frac{j\pi(m-m')}{M}}z^{-2}\times \\ &\quad \sum_{l=0}^{\frac{M}{2}-1} G_l(-z^2)G_{M-1-l}(-z^2)\left\{e^{\frac{2j\pi(m-m')l}{M}} + e^{\frac{2j\pi(m-m')(M-1-l)}{M}}\right\} \\ &= 2(-1)^{(m+m')K+1}j^{m-m'}z^{-2}\times \\ &\quad \sum_{l=0}^{\frac{M}{2}-1} G_l(-z^2)G_{M-1-l}(-z^2)\cos\frac{\pi(m-m')(2l+1)}{M}. \end{aligned} \tag{59}$$

From (59), we deduce that $\mathcal{R}\{j^{-m'}T_2(jz)\} = 0$, if

1. $m-m'$ is odd due to the factor $j^{m-m'}$, the other factors being real,
2. $|m-m'| = \frac{M}{2}$ because all the cosines in the sum are null.

When $|m-m'| = 2r$ with $0 \le r < \frac{M}{4}$, we get

$$\mathcal{R}\{j^{-m'}T_2(jz)\} = -2(-1)^r z^{-2}\sum_{l=0}^{\frac{M}{2}-1} G_l(-z^2)G_{M-1-l}(-z^2)\cos\frac{2\pi(2l+1)r}{M}. \tag{60}$$

We denote by $c_r(-z^2)$ the right member in (60) with

$$c_r(z) = 2(-1)^r z^{-1}\sum_{l=0}^{\frac{M}{2}-1} G_l(z)G_{M-1-l}(z)\cos\frac{2\pi(2l+1)r}{M}. \tag{61}$$

When $|m-m'| = M-2r$ with $0 \le r < \frac{M}{4}$, we get

$$\cos\frac{\pi(m-m')(2l+1)}{M} = \cos\left(\pi(2l+1) - \frac{2\pi(2l+1)r}{M}\right)$$

$$= \quad -\cos\frac{2\pi(2l+1)r}{M},$$

and therefore, from (59), $\mathcal{R}\{j^{-m'}T_2(jz)\} = -c_r(-z^2)$.
Observing that

$$\cos\frac{2\pi(2l+1)r}{M} = \cos\frac{2\pi(2(\frac{M}{2}-1-l)+1)r}{M},$$

and $G_{M-1-l}(z) = s(G_l)(z)$, $G_{\frac{M}{2}-1-l} = s(G_{l+\frac{M}{2}})(z)$, we obtain

$$\begin{aligned} c_r(z) &= 2(-1)^r z^{-1} \sum_{l=0}^{\frac{M}{4}-1} \Big[G_l(z)s(G_l)(z) + G_{l+\frac{M}{2}}(z)s(G_{l+\frac{M}{2}})(z)\Big] \cos\frac{2\pi(2l+1)r}{M} \\ &= b_r(z), \end{aligned}$$

from the definition of $b_r(z)$ by (7).
This proves that $\hat{\boldsymbol{X}}_m(z) = \boldsymbol{T}(z)\,\boldsymbol{X}_m(z)$ with $\boldsymbol{T}(z)$ defined by (47) and achieves the proof of (i).

(ii)– From (i), we get

$$\boldsymbol{T}(z) = \boldsymbol{J}_\sigma\,\boldsymbol{D}_2[\boldsymbol{B}_{\frac{M}{2}}(-z^2)]\,\boldsymbol{J}_\sigma^T, \tag{62}$$

where $\boldsymbol{B}_{\frac{M}{2}}(z)$ is the matrix defined in (20) with $n = \frac{M}{2}$ and $b_r = b_r(-z^2)$, $0 \le r \le \frac{M}{4}-1$. Therefore, from (36), the eigenvalues of $\boldsymbol{T}(z)$ are the elements of the vector

$$\boldsymbol{\mu}_{\frac{M}{4}}(-z^2) = \boldsymbol{C}_{\frac{M}{4}}\;\boldsymbol{b}_{\frac{M}{4}}(-z^2) \text{ with } \boldsymbol{b}_{\frac{M}{4}}(z) = \begin{bmatrix} b_0(z) \\ b_1(z) \\ \dots \\ b_{\frac{M}{4}-1}(z) \end{bmatrix}.$$

Now following (38), $\boldsymbol{C}_{\frac{M}{4}} = 2\boldsymbol{J}_\tau\;\boldsymbol{C}^{III}_{\frac{4}{2}}$, where τ is the permutation of $\{0,1,\dots,\frac{M}{4}-1\}$ of even values in increasing order followed by the list of odd values in decreasing order. From Proposition 1 (i), $\boldsymbol{b}_{\frac{M}{4}}(-z^2) = \frac{4}{M}\,\boldsymbol{\Gamma}_{\frac{M}{4}}\,\boldsymbol{C}^{II}_{\frac{M}{4}}\,\boldsymbol{\lambda}_{\frac{M}{4}}(-z^2)$. Therefore

$$\boldsymbol{\mu}_{\frac{M}{4}}(-z^2) = \frac{8}{M}\boldsymbol{J}_\tau\,\boldsymbol{C}^{III}_{\frac{M}{4}}\,\boldsymbol{\Gamma}_{\frac{M}{4}}\,\boldsymbol{C}^{II}_{\frac{M}{4}}\,\boldsymbol{\lambda}_{\frac{M}{4}}(-z^2).$$

Using Lemma 1 and (3), we get $\boldsymbol{\mu}_{\frac{M}{4}}(-z^2) = \boldsymbol{J}_\tau\,\boldsymbol{J}_{\frac{M}{4}}\,\boldsymbol{\lambda}_{\frac{M}{4}}(-z^2)$, which shows that the elements of $\boldsymbol{\mu}_{\frac{M}{4}}(-z^2)$ are a permutation of the elements of $\boldsymbol{\lambda}_{\frac{M}{4}}(-z^2)$. This proves (ii).

(iii)– We check that $\boldsymbol{J}_\tau\,\boldsymbol{J}_{\frac{M}{4}} = \boldsymbol{J}_{\bar\tau}$ where $\bar\tau$ is the permutation defined in (46).
From (29), we get

$$\begin{aligned} \boldsymbol{B}_{\frac{M}{2}}(z) &= \boldsymbol{R}_{\frac{M}{2}}\,\boldsymbol{D}_2[\boldsymbol{\Delta}(\boldsymbol{\mu}_{\frac{M}{4}}(z))]\,\boldsymbol{R}_{\frac{M}{2}} \\ &= \boldsymbol{R}_{\frac{M}{2}}\,\boldsymbol{D}_2[\boldsymbol{\Delta}(\boldsymbol{J}_{\bar\tau}\boldsymbol{\lambda}_{\frac{M}{4}}(z))]\,\boldsymbol{R}_{\frac{M}{2}} \\ &= \boldsymbol{R}_{\frac{M}{2}}\,\boldsymbol{D}_2[\boldsymbol{J}_{\bar\tau}\boldsymbol{\Delta}(\boldsymbol{\lambda}_{\frac{M}{4}}(z))\boldsymbol{J}_{\bar\tau}^T]\,\boldsymbol{R}_{\frac{M}{2}} \end{aligned}$$

using (4). Then, from (54), it comes

$$\begin{aligned}\boldsymbol{T}(z) &= \boldsymbol{J}_\sigma\, \boldsymbol{D}_2[\boldsymbol{R}_{\frac{M}{2}}\, \boldsymbol{D}_2[\boldsymbol{J}_{\bar\tau}\, \boldsymbol{\Delta}(\boldsymbol{\lambda}_{\frac{M}{4}}(-z^2))\boldsymbol{J}_{\bar\tau}^T]\, \boldsymbol{R}_{\frac{M}{2}}]\, \boldsymbol{J}_\sigma^T, \\ &= \boldsymbol{J}_\sigma\, \boldsymbol{D}_2[\boldsymbol{R}_{\frac{M}{2}}]\, \boldsymbol{D}_4[\boldsymbol{J}_{\bar\tau}]\, \boldsymbol{D}_4[\boldsymbol{\Delta}(\boldsymbol{\lambda}_{\frac{M}{4}}(-z^2))]\, \boldsymbol{D}_4[\boldsymbol{J}_{\bar\tau}^T]\, \boldsymbol{D}_2[\boldsymbol{R}_{\frac{M}{2}}]\, \boldsymbol{J}_\sigma^T. \end{aligned} \tag{63}$$

The result for (iii) follows.

(iv)– The matrix $\boldsymbol{T}(z)$ has the form $\beta z^{-n}\, \boldsymbol{I}_M$ for a non null constant β if and only if any eigenvalue $\lambda_r(-z^2) = \beta z^{-n},\ 0 \le r \le \frac{M}{4} - 1$. Because $\lambda_r(z)$ has the form $\lambda_r(z) = z^{-1}q(z)$ where $q(z)$ is a polynomial in z^{-1} of degree $2K-2$ with $z^{-(2K-2)}q(1/z) = q(z)$, this implies that $\lambda_r(z) = \alpha\, z^{-K}$, and therefore $\lambda_r(-z^2) = (-1)^K \alpha\, z^{-2K}$. From Proposition 2-(ii), this is equivalent to the PR property of the prototype filter $P(z)$ with $\alpha = \|P(z)\|_2^2$ and $\beta = (-1)^K\alpha$. □

4.2 The FBMC/OQAM interference function

According to Theorem 3, when the prototype filter is PR, the detected sequence is an exact reproduction, up to a time offset, of the transmitted sequence. When the prototype filter is no longer PR, we need a quantitative measurement of its distance to perfect reconstruction, i.e. the *interference function* of the prototype filter.
Transmitting the $\boldsymbol{X}(z)$ sequence always results in the detection of $\hat{\boldsymbol{X}}(z)$, a sequence which is equal to $(-1)^K\alpha z^{-2K}\boldsymbol{X}(z)$ for a PR TMUX system. The difference is therefore equal to $\boldsymbol{Y}(z) = [\boldsymbol{T}(z) - (-1)^K\alpha z^{-2K}\boldsymbol{I}_M]\, \boldsymbol{X}(z)$.

To define a norm for matrix $\boldsymbol{A}(z) = \boldsymbol{T}(z) - (-1)^K\alpha z^{-2K}\boldsymbol{I}_M$, we first need a norm of its elements.
A first possible choice is to consider the l^1 norm on polynomials in z^{-1}: if $q(z) = \sum_n q[n]z^{-n}$, then $\|q(z)\|_1 = \sum_n |q[n]|$ and then

$$\|\boldsymbol{A}(z)\| = \sup\{\sum_{c=0}^{M-1} \|\boldsymbol{A}_{r,c}(z)\|_1,\ 0 \le r \le M-1\}. \tag{64}$$

For the considered TMUX, up to a sign change, any line of $\boldsymbol{A}(z)$ contains the same non null elements, and

$$\begin{aligned}\|\boldsymbol{A}(z)\| &= \|b_0(-z^2) - (-1)^K z^{-2K}\|_1 + 2\sum_{c=0}^{\frac{M}{4}-1} \|b_r(-z^2)\|_1 &(65)\\ &= \|b_0(z) - z^{-K}\|_1 + 2\sum_{c=0}^{\frac{M}{4}-1} \|b_r(z)\|_1. &(66)\end{aligned}$$

This is the choice made in [7] for example.

Another choice is to consider the l^2 norm on filters $q(z) = \sum_n q[n]z^{-n}$ defined by

$$\|q(z)\|_2^2 = \sum_n |q[n]|^2 = \int_0^1 \left|q\left(e^{2j\pi\nu}\right)\right|^2\, d\nu, \tag{67}$$

and then the interference is expressed using Frobenius norm $\|\boldsymbol{A}(z)\|_F$ defined by

$$\|\boldsymbol{A}(z)\|_F^2 = \sum_{r,c=0}^{M-1} \|[\boldsymbol{A}]_{r,c}(z)\|_F^2. \tag{68}$$

This definition is chosen in [24], [20], [25] for example. Furthermore, as illustrated in [26, 27], an adaption of the Frobenius norm of the ambiguity function could also be used to derive the Signal to Interference Ratio (SIR) in the case of FBMC/OQAM transmission through time and frequency dispersive channels. We, therefore here, choose to focus on this norm.

Using the notations of the first paragraph, we introduce the following definition.

Definition 1. *Given $K \geq 3$, $M \geq 4$ multiple of 4, $P(z)$ a symmetric prototype filter of length $L = KM$, and the TMUX defined by $P(z)$, as in Figure 1 with transfer matrix $\boldsymbol{T}(z)$, then the* interference function $I(P)$ *is defined by*

$$I(P) = \frac{1}{M\alpha^2} \|\boldsymbol{T}(z) - (-1)^K \alpha z^{-2K} \boldsymbol{I}_M\|_F^2 \text{ with } \alpha = \|P(z)\|_2^2. \tag{69}$$

The next proposition shows that $I(P)$ may be expressed in different equivalent ways, the expression (72) in terms of matrix $\boldsymbol{W}$ elements being the most practical for calculations.

Proposition 4. *Let $K \geq 3$, $M \geq 4$ a multiple of 4 and $P(z)$ a symmetric real prototype filter $P(z)$ of length $L = KM$. With the definitions of section 2, the following properties are verified*

$$(i) \quad I(P) = \frac{1}{\alpha^2} \left(\|b_0(z) - \alpha z^{-K}\|_2^2 + 2 \sum_{r=1}^{\frac{M}{4}-1} \|b_r(z)\|_2^2 \right), \tag{70}$$

$$(ii) \quad I(P) = \frac{4}{M\alpha^2} \sum_{r=0}^{\frac{M}{4}-1} \|\lambda_r(z) - \alpha z^{-K}\|_2^2. \tag{71}$$

$$(iii) \quad I(P) = \frac{2}{[\boldsymbol{W}]_{0,0}^2} \left(\sum_{c=1}^{K-1} [\boldsymbol{W}]_{0,c}^2 + \sum_{r=1}^{\frac{M}{4}-1} [\boldsymbol{W}]_{r,0}^2 + 2 \sum_{r=1}^{\frac{M}{4}-1} \sum_{c=1}^{K-1} [\boldsymbol{W}]_{r,c}^2 \right), \tag{72}$$

$$(iv) \quad I(P) = \frac{M}{\alpha^2} \sum_{r=0}^{\frac{M}{4}-1} \left[\left([\boldsymbol{V}]_{r,0} - \frac{2\alpha}{M} \right)^2 + 2 \sum_{c=1}^{K-1} [\boldsymbol{V}]_{r,c}^2 \right]. \tag{73}$$

Proof.– (i)– Each row of matrix $\boldsymbol{T}(z)$ contains $b_0(-z^2)$ and two copies of $b_r(-z^2)$, $1 \leq r \leq \frac{M}{4} - 1$, with a sign ± 1. This proves (i) because $\|q(-z^2)\|_2^2 = \|q(z)\|_2^2$ for any polynomial $q(z)$ in z^{-1}.

(ii)– From equation (48), we deduce that

$$\boldsymbol{T}(z) - (-1)^K \alpha z^{-2K} = \boldsymbol{U}\, \boldsymbol{D}_4 \left[\boldsymbol{\Delta}(\boldsymbol{\lambda}_{\frac{M}{4}}(-z^2) - (-1)^K \alpha \boldsymbol{I}_{\frac{M}{4}}\, z^{-2K}) \right] \boldsymbol{U}^T. \tag{74}$$

On another hand, for an $N \times N$ polynomial matrix $\boldsymbol{A}(z) = \sum_n \boldsymbol{A}_n z^{-n}$ where the $\boldsymbol{A}_n$ are constant matrices, and for an $N \times N$ orthogonal constant matrix $\boldsymbol{U}$, we get

$$\boldsymbol{U}^T\, \boldsymbol{A}(z)\, \boldsymbol{U} = \sum_n \boldsymbol{U}^T\, \boldsymbol{A}_n\, \boldsymbol{U}\, z^{-n}. \tag{75}$$

Because

$$\|\boldsymbol{U}^T\,\boldsymbol{A}_n\,\boldsymbol{U}\|_2^2 = \|\boldsymbol{A}_n\|_2^2, \tag{76}$$

and

$$\|\boldsymbol{A}(z)\|_F^2 = \sum_n \|\boldsymbol{A}_n\|_2^2, \tag{77}$$

we get

$$\|\boldsymbol{T}(z) - (-1)^K \alpha z^{-2K}\|_F^2 \;\; = \;\; \|\boldsymbol{D}_4 \left[\boldsymbol{\Delta}(\boldsymbol{\lambda}_{\frac{M}{4}}(-z^2) - (-1)^K \alpha \boldsymbol{I}_{\frac{M}{4}} z^{-2K}\right]\|_F^2, \tag{78}$$

which proves (ii).

(iii) is straightforward proved using (i) and equation (18) while (iv) is proved using (ii) and equation (14).

□

Remark 5. *With the previous definitions, changing $P(z)$ to a proportional filter $kP(z)$ multiply the functions $\|P(z)\|_2^2$, $b_r(z), \lambda_r(z)$, and the matrix $T(z)$ of the MUX by the constant k^2. Therefore the interference function is not modified: $I(kP) = I(P)$, as it is the case for other optimization cost functions.*

As in [9], the interference function $I(P)$ may be used as an optimizing criterion (criterion C4 where the interference function is denoted TOI for *TOtal Interference*) to design prototype filters $P(z)$. In the following paragraphs, the notation TOI is used.

5 Comparison of various nearly PR prototype filters

A large number of textbooks and publications clearly illustrate the fact that communication system designers are often attracted by filters, or prototype filters, that only involve a limited number of parameters. Furthermore, even if the PR property provides some implementation advantages, often also nearly PR solutions are preferred. In this respect, the simplicity of the *Square Root Raised Cosine (SRRC)* filter makes it a permanent reference in the field. In the case of FBMC/OQAM systems, the prototype filters either based on the Martin and Mirabassi design method [12] or, nearly equivalently, on the frequency sampling approach proposed by M. Bellanger [13], also still reach a large audience due to their high frequency selectivity combined with a nearly PR property. Let denominate this prototype filter as the MMB prototype. On another hand, the importance of time-frequency localization for transmission through time-frequency selective channels makes the Isotropic Orthogonal Transform Algorithm (IOTA) [6] and the Extended Gaussian Function (EGF) [15] very appealing. But the number of EGF parameters may become high according to the required accuracy.
Thus in this section we propose an EGF variant only involving a reduced number of parameters and another new family of prototype filters combining the proposed EGF variant with the MMB prototype filter. But let us start with the SRRC prototype.

5.1 SRRC prototype filters

If the SRRC function has been optimized for various single carrier settings, as illustrated recently in [28] and [29], in the case of FBMC/OQAM, to the best of our knowledge, the authors only use it with predetermined roll-off values, as the case still recently in reference [30], often selecting, as in [31], the widest possible transition band.
The SRRC continuous function ([32]) of real variable t is defined, for a given roll-off r, $0 \leq r \leq 1$ and a frequency bandwidth in the range $[-F, F]$, by

$$r_C(t) = \frac{4rFt\cos(\pi(1+r)Ft) + \sin(\pi(1-r)Ft)}{\sqrt{F}\pi t(1-16F^2r^2t^2)}, \tag{79}$$

if the denominator does not vanish and extended by continuity otherwise, i.e.

$$r_C(0) = \sqrt{F}\left(1 - r + \frac{4r}{\pi}\right),$$
$$r_C\left(\pm\frac{1}{4rF}\right) = \frac{\sqrt{2F}}{2\pi}\, r\left[(\pi-2)\cos\left(\frac{\pi}{4r}\right) + (\pi+2)\sin\left(\frac{\pi}{4r}\right)\right].$$

For $K \geq 3$ and $M \geq 4$ multiple of 4, the SRRC filter $P(z)$ of length $L = KM$ is obtained by setting, F, the FBMC/OQAM frequency spacing, such as $F = \frac{1}{M}$ and

$$P(z) = \sum_{n=0}^{L-1} p[n]z^{-n},\ p[n] = r_C\left(\frac{2n+1-L}{2}\right),\ 0 \leq n \leq L-1. \tag{80}$$

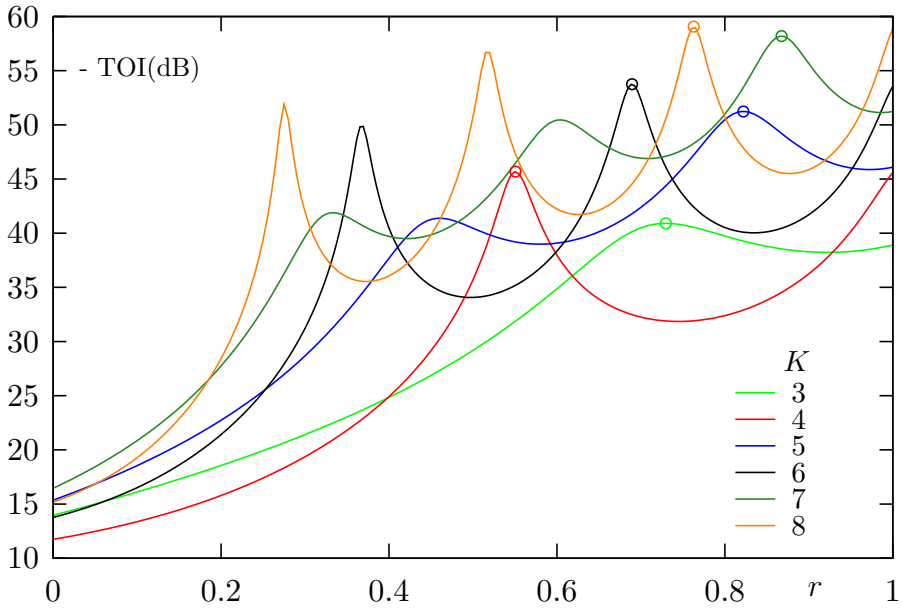

Figure 2: TOI value as a function of $r,\ 0 \leq r \leq 1$, for the SRRC filters with $3 \leq K \leq 8$ and $M = 64$.

For $3 \leq K \leq 8$ and $M = 64$, Figure 2 shows the variation of -TOI(dB) as a function of r for $0 \leq r \leq 1$. The maximum value of -TOI(dB) for each value of K is indicated by a circle symbol.
In Figure 2 it is worth noting that, according to the overlapping factor, e.g. for $K = 5$ and 7, TOI gains above 5 dB are attained when selecting the optimal r value instead of the most frequently selected one, i. e. $r = 1$.
Table 1 gives the main characteristic constants of the SRRC filters optimized for the Total Interference TOI: the value of r_{opt} that gives the maximum -TOI(dB), the corresponding values of -TOI(dB), -E(dB), where E is the out-of-band energy, and TFL the time-frequency localization measure, a real value going from 0 to 1 for the worst to the best, as defined for instance in [7] for discrete-time filters.
Note also that the results in Table 1 are consistent with the ones reported in [7, Table I] for the l^1 norm (66) where it also appeared that, among the three tested roll-off values (1/2, 3/4,1) , $r = 1$ was not always the best choice. On the contrary, it can be easily checked that if the SRRC optimization is carried out with respect to the TFL criterion, $r = 1$ always leads to the optimum solution with a maximum of 0.9004 attained for $K = 4$ when $M = 64$.

K	r_{opt}	- TOI(dB)	- E(dB)	TFL
3	0.729686	40.91	37.23	0.8684
4	0.550574	45.69	37.47	0.7799
5	0.821964	51.24	44.44	0.8721
6	0.689446	53.75	45.05	0.8316
7	0.867511	58.19	49.05	0.8746
8	0.762957	59.07	49.96	0.8489

Table 1: Optimal SRRC prototype filters for TOI, $3 \leq K \leq 8$ and $M = 64$.

5.2 A new variant of EGF prototype filters

For $\lambda > 0$ and $\tau_0 > 0, \nu_0 > 0$ such that $\nu_0\tau_0 = \frac{1}{2}$, we consider the real continuous-time function $z_{\lambda,\nu_0,\tau_0}(t)$ of the real time variable t defined by

$$z_{\lambda,\nu_0,\tau_0}(t) = \frac{1}{2}\left[\sum_{k=0}^{\infty} c_k \left[g_\lambda(t + \frac{k}{\nu_0}) + g_\lambda(t - \frac{k}{\nu_0})\right]\right] \times \left[\sum_{l=0}^{\infty} d_l \cos\left(2\pi l \frac{t}{\tau_0}\right)\right], \qquad (81)$$

where $g_\lambda(t) = (2\lambda)^{\frac{1}{4}} e^{-\lambda\pi t^2}$ and $c_k, d_k,\ k \geq 0$, are real coefficients. In the FBMC/OQAM context, (81) and (79) are connected by the equalities $\nu_0 = F$ and $\tau_0 = \frac{1}{2F}$, real symbol duration, with $\nu_0\tau_0 = \frac{1}{2}$.
This function, called the *Extended Gaussian Function (EGF)*, was first introduced and studied in [14], [15], [16].
In this paragraph, we consider discrete-time filters obtained in the following way. First, a very special case of the continuous-time function (81) is selected where the second sum is reduced to a constant, i.e. $d_0 = 2$ and $d_k = 0,\ k \geq 1$. Then the first sum is restricted to K

terms with coefficients $c_k,\ 0 \leq k \leq K-1$, for a given $K \geq 2$. Thus, we obtain the real-time function $z_{\lambda,a}(t)$ defined by

$$z_{\lambda,a}(t) = \sum_{k=0}^{K-1} c_k \left[g_\lambda(t+ak) + g_\lambda(t-ak) \right]. \tag{82}$$

As we also need to consider the case $\lambda = 0$ while restricting λ, as factor in the exponential argument, to be a positive constant, we define the function $\bar{g}_\lambda(t) = e^{-\lambda^2 \pi t^2}$ and the function $\bar{z}_{\lambda,a}(t)$ by

$$\bar{z}_{\lambda,a}(t) = \sum_{k=0}^{K-1} c_k \left[\bar{g}_\lambda(t+ak) + \bar{g}_\lambda(t-ak) \right]. \tag{83}$$

For $M \geq 4$, multiple of 4, a regular sampling of $(2\tilde{\lambda})^{-\frac{1}{4}} z_{\tilde{\lambda},\tilde{a}}(t)$ with $L = KM$ points, $y_n,\ 0 \leq n < L$, in the interval $(-\frac{K}{2}, \frac{K}{2})$, defined by

$$y_n = K\left(\frac{2n+1}{2L} - \frac{1}{2}\right) \tag{84}$$

is equivalent to the sampling in the interval $(-\frac{1}{2}, \frac{1}{2})$ of $\bar{z}_{\lambda,a}(t)$ with the L points $x_n,\ 0 \leq n < L$, defined by

$$x_n = \frac{2n+1}{2L} - \frac{1}{2}, \tag{85}$$

if

$$\tilde{\lambda} = \frac{\lambda^2}{K^2},\ \tilde{a} = Ka. \tag{86}$$

We therefore consider the symmetric prototype filter $P(z) = \sum_{n=0}^{L-1} \bar{z}_{\lambda,a}(x_n) z^{-n}$ and we look for values of λ, a and $c_k,\ 0 \leq k \leq K-1$ that provide a filter with good frequency characteristics and minimal TOI.
As this EGF variant corresponds to a linear combination of Gaussian functions, or Gaussian filters, we name this new family of functions and/or prototype filters using the acronym LCGF.

For given values of K and M, the optimization process with variables λ, a and $c_k,\ 0 \leq k \leq K-1$ is very difficult because there is a lot of local minima. As an example, for $K = 3$ and $M = 64$, for a fixed value of λ, $1.5 \leq \lambda \leq 20.5$, we get a minimum of TOI, represented in Figure 3 by -TOI(dB) as a function of λ in the blue curve. For $\lambda = \lambda_1 = 3.969156$, a maximum -TOI(dB) = 51.33 value is obtained, which is a local maximum of -TOI(dB). For $\lambda = \lambda_3 = 12.4060$, we get -TOI(dB) = 79.14 which seems to be a global maximum for -TOI(dB). However, for $\lambda = \lambda_1$, the out-of-band energy is $E = 8.11 \times 10^{-5}$ while $E = 6.54 \times 10^{-2}$ for $\lambda = \lambda_3$. The characteristics of these two filters are represented in Figures 4 and 5.
Therefore, in order to get a local TOI optimum with an acceptable out-of-band energy, for $4 \leq K \leq 8$, as for $K = 3$, the value of λ is constrained by some bound. Table 2 gives the main characteristics of the obtained local optimal prototype filters.
In the comparison between the SRRC and LCGF prototype filters, it appears that with the LCGF an overlapping of $K = 3$ is sufficient to outperform a nettly much longer, with $K = 5$, SRRC with regard to the three measures considered : TOI, E and TFL.

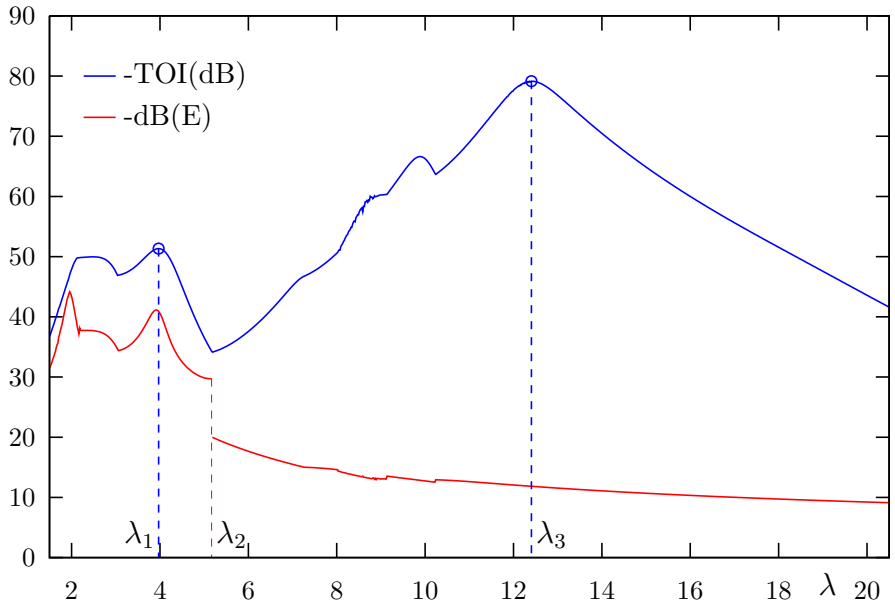

Figure 3: TOI optimization for LCGF with $K = 3$, $M = 64$ and $1.5 \leq \lambda \leq 20.5$.

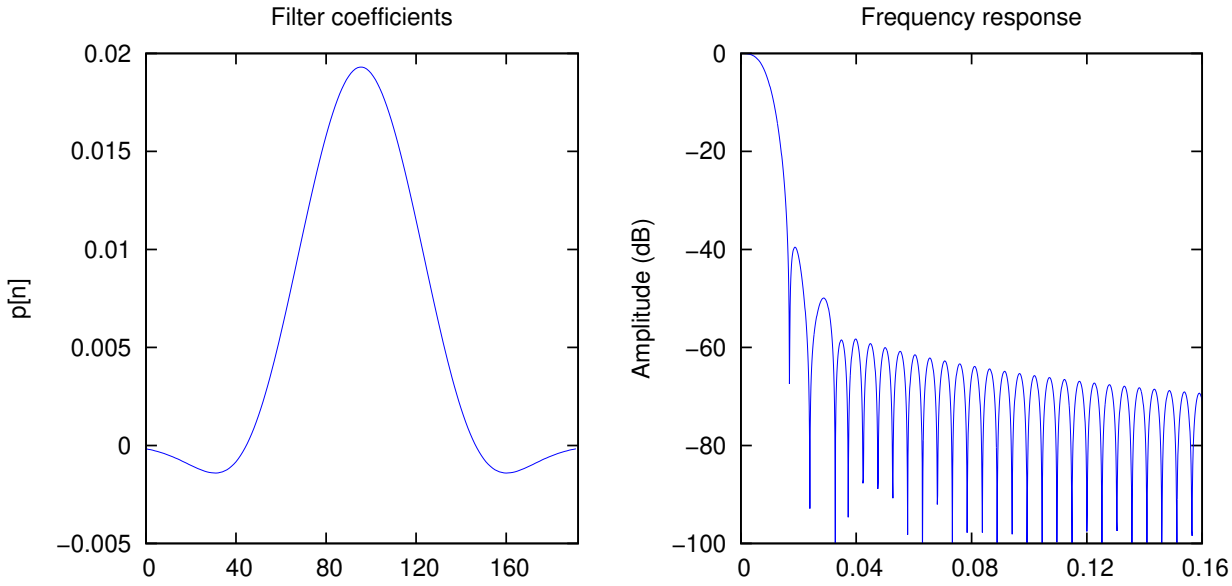

Figure 4: LCGF with $K = 3$, $M = 64, \lambda = \lambda_1 = 3.969156$ with optimal TOI: -TOI(dB) = 51.333252.

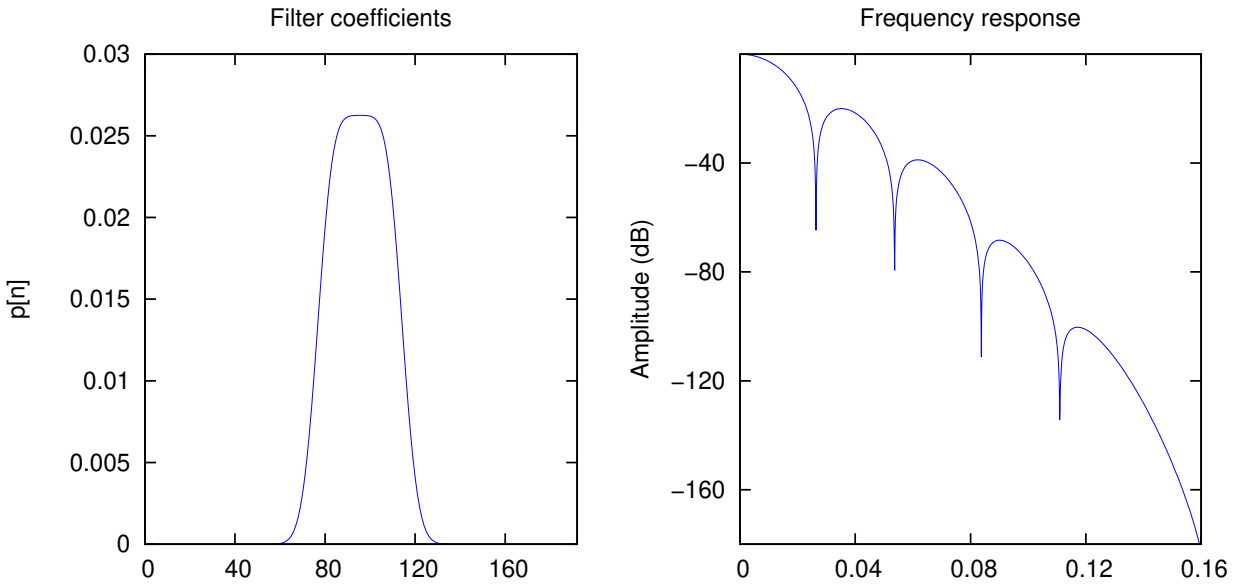

Figure 5: LCGF with $K = 3$, $M = 64, \lambda = \lambda_3 = 12.4060$ with optimal TOI: -TOI(dB) = 79.142708.

K	λ_{opt}	a_{opt}	- TOI(dB)	- E(dB)	TFL
3	3.96916	1.301623×10^{-1}	51.33	40.91	0.9118
4	4.16950	9.818990×10^{-2}	70.60	44.94	0.9054
5	4.46048	7.964676×10^{-2}	84.39	50.77	0.8775
6	4.38281	1.173788×10^{-1}	86.17	52.90	0.8493
7	4.99656	9.968591×10^{-2}	89.71	57.06	0.8281
8	5.42586	8.838837×10^{-2}	96.47	62.72	0.8140

Table 2: Characteristics of optimized LCGF prototype for the interference criterion (TOI), $3 \leq K \leq 8$, $M = 64$).

K	3	4	5
c_1	8.684747×10^{-1}	5.751089×10^{-1}	3.793495×10^{-1}
c_2	-4.148046×10^{-1}	-5.942950×10^{-1}	-7.104150×10^{-1}
c_3	—	9.721558×10^{-2}	1.515300×10^{-1}
c_4	—	—	5.912280×10^{-3}
K	6	7	8
c_1	-7.185977×10^{-1}	-7.208048×10^{-1}	-8.196402×10^{-1}
c_2	1.846397×10^{-1}	1.466245×10^{-1}	2.120102×10^{-1}
c_3	-5.350222×10^{-2}	-1.307413×10^{-2}	-4.116862×10^{-2}
c_4	2.427846×10^{-2}	-2.313501×10^{-3}	9.141708×10^{-3}
c_5	-1.336278×10^{-2}	2.624612×10^{-3}	-3.796928×10^{-3}
c_6	—	-3.582594×10^{-3}	2.880454×10^{-3}
c_7	—	—	-3.875055×10^{-3}

Table 3: Coefficients $c_k,\ 1 \leq k \leq K-1,\ 3 \leq K \leq 8$, of the LCGF prototype filter optimized for TOI with $c_0 = 1$ ($M = 64$).

5.3 A more general class of EGF prototype filters

In this subsection, a more general class of EGF prototype filters, here denoted by *GENeral EGF filters* (abbreviated by GEN), is introduced that contains the MMB prototype filters such as described in [12] and [20] and the LCGF described in the previous subsection.
For a given value of $K \geq 3$, the generating prototype function for the GEN class is the real continuous-time function $z(t)$ defined by

$$z(t) = \left[\sum_{k=0}^{K-1} c_k \left[\bar{g}_\lambda(t + ak) + \bar{g}_\lambda(t - ka)\right]\right] \times \left[\sum_{l=0}^{K-1} d_l \cos(2\pi\,\beta\,l\,(2t+1))\right], \tag{87}$$

depending on the $2K + 3$ parameters $\lambda, a, c_k,\ 0 \leq k \leq K-1,\ \beta$ and $d_l,\ 0 \leq l \leq K-1$.

For $d_0 = 1$ and $d_l = 0,\ 1 \leq l \leq K-1,\ z(t)$ generates by a sampling at the points $x_n = \frac{2n+1}{2L} - \frac{1}{2},\ 0 \leq n \leq KM-1$ the EGF prototypes of length $L = KM$.
With the same time-discretization points, and $\lambda = 0$, $C = 2\sum_{k=0}^{K-1} c_k \neq 0$ and $\beta = 1$, the $P(z)$ filters are given, up to the multiplicative constant C, by

$$P(z) = \sum_{n=0}^{L-1} p[n] z^{-n}, \tag{88}$$

with

$$p[n] = \sum_{l=0}^{K-1} d_l \cos(2\pi l y_n),\ y_n = \frac{2n+1}{2L},\ 0 \leq n \leq L-1, \tag{89}$$

which is the definition given by equation (6) in [12] and in the Phydyas project [20]. There is however a slight modification of coefficients d_l ($d_0 = k_0$ and $d_l = 2k_l,\ 1 \leq l \leq K-1$),

a different multiplicative constant and an adaption of the discretization points to get a symmetric prototype filter with even length.
For $3 \leq K \leq 5$, Tables 4, 5 and 6 compare the characteristics of the prototype filters, obtained by optimization of the TOI criterion with $M = 64$:

1. SRRC: the Square Root Raised Cosine filter described in subsection 5.1,
2. MMB: the Mirabassi-Martin-Bellanger filter such as described in [20] (Phydyas filters), with an even length,
3. LCGF: the Linear Combination of Extended Gaussian Filters described in subsection 5.2,
4. GEN: the prototype filter described in this subsection.

Figure 6, 7 and 8 show the frequency curves of these filters. However, in Figure 8, the frequency curve of the GEN filter is not plotted because it is almost identical to the one of the LCGF prototype.

	- TOI(dB)	- E(dB)	TFL
SRRC	40.91	37.23	0.8684
MMB	46.25	39.78	0.8844
LCGF	51.33	40.91	0.9118
GEN	57.36	36.64	0.9307

Table 4: Characteristics comparison of prototype filters SRRC, MMB, LCGF and GEN optimized for TOI criterion with $K = 3$ and $M = 64$.

	- TOI(dB)	- E(dB)	TFL
SRRC	45.69	37.47	0.7799
MMB	67.20	43.89	0.8866
LCGF	70.60	44.94	0.9054
GEN	74.12	46.63	0.9070

Table 5: Characteristics comparison of prototype filters SRRC, MMB, LCGF and GEN optimized for TOI criterion with $K = 4$ and $M = 64$.

Our MMB prototypes optimizations are carried out over $K - 1$ coefficients, simply setting $c_0 = 1$, while in [20], the authors only take advantage of one degree of freedom for $K = 3$ and 4 and only of 2 for $K = 5$. By the way, compared to [20], we obtain a TOI improvement ranging from 0.75 dB, for $K = 3$ to more than 9 dB for $K = 5$. Our comparisons reported in Tables 4-6 between all the prototype filters focus on the three most commonly used overlapping factors, i. e. $K = 3$, 4 or 5. These tables clearly show that the new families of prototype filters we have introduced outperform the SRRC and MMB solutions with TOI

	- TOI(dB)	- E(dB)	TFL
SRRC	51.24	44.44	0.8721
MMB	80.96	61.07	0.8423
LCGF	84.39	50.77	0.8775
GEN	84.88	51.24	0.8767

Table 6: Characteristics comparison of prototype filters SRRC, MMB, LCGF and GEN optimized for TOI criterion with $K = 5$ and $M = 64$.

K	3	4	5
λ	2.237626	1.950356	4.459006
a	-2.832273×10^{-1}	4.361842×10^{-1}	7.951699×10^{-2}
c_1	1.286036	-2.128282×10^{-1}	3.785814×10^{-1}
c_2	1.106024×10^{-2}	4.383833×10^{-1}	-7.096004×10^{-1}
c_3	—	1.154026×10^{-1}	1.505152×10^{-1}
c_4	—	—	6.395659×10^{-3}
β	1.002248	6.578910×10^{-1}	9.992112×10^{-1}
d_1	-9.871248×10^{-1}	-4.712546×10^{-1}	1.052062×10^{-3}
d_2	-4.259598×10^{-1}	-3.566996×10^{-1}	-2.381287×10^{-3}
d_3	—	7.317746×10^{-1}	-8.112096×10^{-4}
d_4	—	—	-1.370125×10^{-4}

Table 7: Coefficients of the GEN prototype filter optimized for TOI with $c_0 = d_0 = 1$ ($M = 64$).

improvements w.r.t. the optimized MMB ranging for the GEN solution between 3.92 ($K = 5$) and 17.85 ($K = 3$) dB. The new families of prototypes also lead to better TFL measures. Results, not reported here, have shown that up to $M = 2048$, keeping the optimized coefficients as for $M = 64$, lead to similar performance measures.

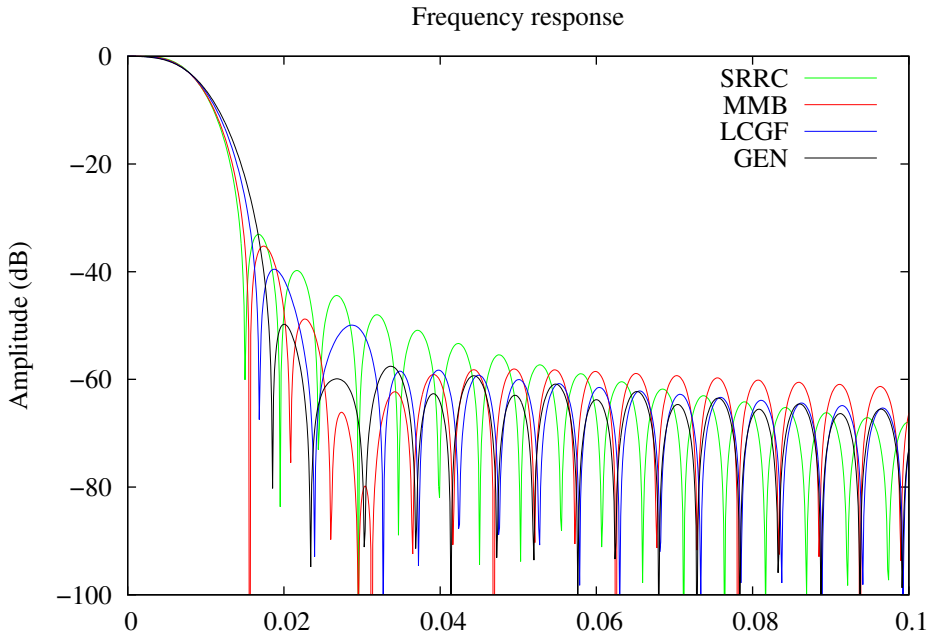

Figure 6: Comparison of characteristics of prototype filters for $K = 3$, $M = 64$: SRRC, MMB, LCGF and GEN filters optimized for TOI.

6 Conclusion

In this note we have revisited the analysis and design problem of symmetrical FBMC/OQAM system. We have assumed the number M of its subcarrier is a multiple of 4 while the length of its prototype filter is expressed as $L = KM$, with K the integer overlapping factor. Then, some simplifications happen and a new useful description is readily obtained using standard tools from the linear algebra theory. By the way, several equivalent forms of the PR and NPR properties are derived together with a diagonalization of the FBMC/OQAM transfer matrix. On another hand, two new families of prototype filters are introduced that only involve a few parameters. The first one, named LCGF, takes its roots from the EGF, see e.g. [15]. The second one, named GEN, results from a combination of the LCGF with the famous prototype filter introduced, independently, in [11, 12], [13], named here MMB. Our design comparisons have included four families of prototype filters: SRRC, MMB, LCGF and GEN. For an optimization criterion, which is the minimization of the total interference, we showed that, slightly increasing the degree of freedom, setting it to $K + 1$ for the LCGF,

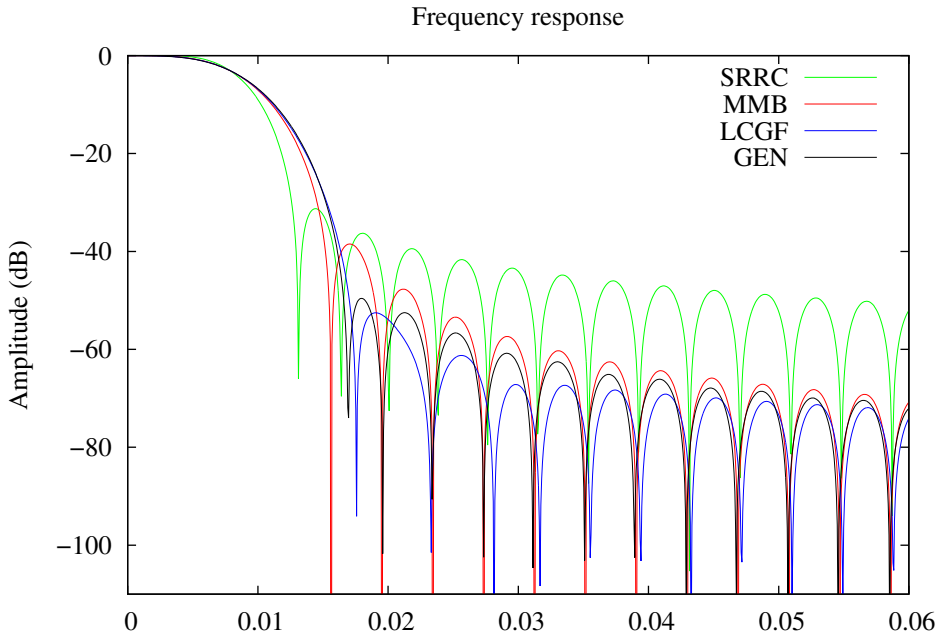

Figure 7: Comparison of characteristics of prototype filters for $K = 4,\ M = 64$: MMB filter, and SRRC, LCGF and GEN filters optimized for TOI.

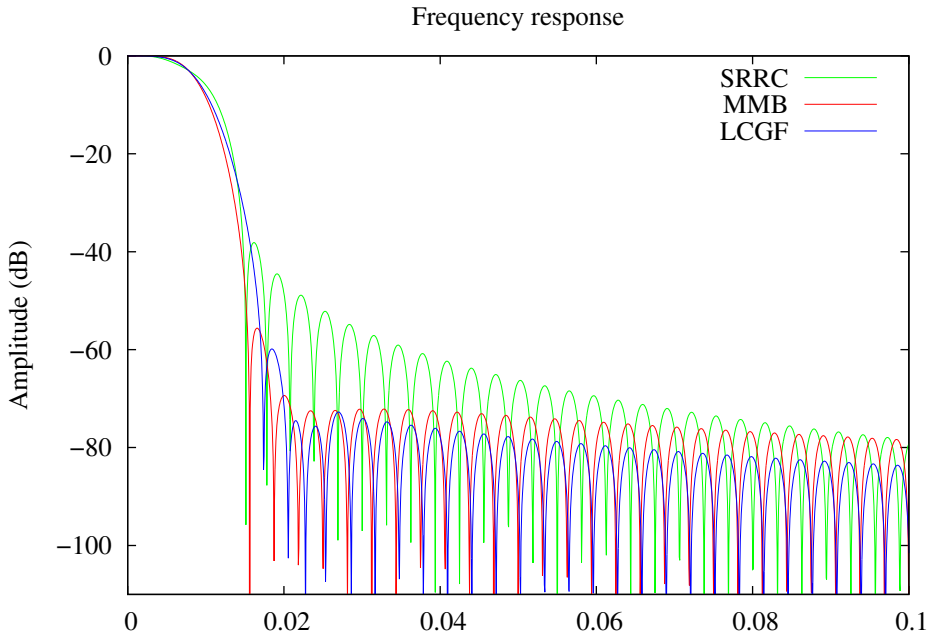

Figure 8: Comparison of characteristics of prototype filters for $K = 5,\ M = 64$: MMB filter, and SRRC and LCGF optimized for TOI.

and to $2K+1$ for GEN, instead of $K-1$ for MMB and 1 for the the SRRC, allowed us to get significantly better design results.

References

[1] R. Nissel, S. Schwarz, and M. Rupp. Filter bank multicarrier modulation schemes for future mobile communications. *IEEE Journal on Selected Areas in Communications*, 35(8):1768–1782, 2017.

[2] M. Renfors and al. (eds). *Orthogonal waveforms and filter banks for future communications*. Academic Press, 2017. xxvii + 555 pages.

[3] B. R. Saltzberg. Performance of an efficient parallel data transmission system. *IEEE Transactions on Communication Technology*, 15(6):805–811, December 1967.

[4] B. Farhang-Boroujeny and C. Yuen. Cosine modulated and offset QAM filter bank multicarrier techniques: A continuous-time prospect. *EURASIP Journal on Advances in Signal Processing*, 2010(8):1–16, 2010.

[5] A. Stevens, T. Sibbett, J. Driggs, H. Moradi, and B. Farhang-Boroujeny. Spread spectrum technique using staggered multi-tone. In *2020 International Conference on Computing, Networking and Communications (ICNC)*, pages 326–331, 2020.

[6] B. Le Floch, M. Alard, and C. Berrou. Coded Orthogonal Frequency Division Multiplex. *Proceedings of the IEEE*, 83:982–996, June 1995.

[7] P. Siohan, C. Siclet, and N. Lacaille. Analysis and design of OFDM/OQAM systems based on filterbank theory. *IEEE Trans. Sig. Proc.*, 50(5):1170–1183, 2002.

[8] European Union 7th Framework Programme: Project PHYDYAS. http://www.ict-phydyas.org.

[9] A. Viholainen, T. Ihalainen, *et al.* Prototype filter design for filter bank based multicarrier transmission. In *Proc. 17th European Signal Porcessing Conference (EUSIPCO'2009), Glasgow, Scotland*, pages 1–5, 2009.

[10] Li Zhongnian and Liu Shouyin. Novel matrix representation for OFDM/OQAM systems. *The Journal of China Universities of Posts and Telecommunications*, 25(3), 2018.

[11] K.W. Martin. Small side-lobe filter design for multitone data-communication applications. *IEEE Trans. on Circuits and Systems II: Analog and Digital Signal Processing*, 45(8):1155–1161, 1998.

[12] S. Mirabbasi and K.W. Martin. Overlapped complex-modulated transmultiplexer filters with simplified design and superior stopbands. *IEEE Trans. on Circuits and Systems II: Analog and Digital Signal Processing*, 50(8):456–469, 2003.

[13] M.G. Bellanger. Specification and design of a prototype filter for filter banks based on multicarrier transmission. In *Proc. 2001 IEEE Intern. Conf. on Acoustics, Speech, and Signal Processing*, volume 4, pages 2417–2420, 2001.

[14] C. Roche and P. Siohan. A family of Extended Gaussian Functions with a nearly optimal localization property. In *Proc. First Int. Workshop on Multi-Carrier Spread-Spectrum (Oberfaffenhofen, Germany)*, pages 179–186, 1997.

[15] P. Siohan and C. Roche. Cosine-modulated filterbanks based on Extended Gaussian Function. *IEEE Trans. Sig. Proc.*, 48(11):3052–3061, 2000.

[16] P. Siohan and C. Roche. Derivation of Extended Gaussian Functions based on the Zak transform. *IEEE Sig. Proc. Letters*, 11(3):401–403, 2004.

[17] V. Britanak, P.C. Yip, and K.R. Rao. *Discrete cosine transforms: Algorithms,Advantages, Applications*. Academic Press, 2006. xiv + 349 pages.

[18] J. J. Benedetto, I. Konstantinidis, and M. Rangaswamy. Phase-coded waveforms and their design. *IEEE Signal Processing Magazine*, 26(1):22–31, Jan 2009.

[19] H.S. Malvar. Modulated QMF filter banks with perfect reconstruction. *Electronic Letters*, 26(13):906–907, 1990.

[20] A. Viholainen, M.G. Bellanger, and M. Huchard. Prototype filter and structure optimization. Technical report, PHYDYAS, 2009. Project deliverable nb D5-1-1, PHYDYAS_007, 102 pages.

[21] G.H. Golub and Ch.F. Van Loan. *Matrix computations*. John Hopkins, 4th. edition, 2013. xxi + 756 pages.

[22] V. Pan. *Structured matrices and polynomials: Unified superfast algorithms*. Springer Science & Business Media, 2001. 278 pages.

[23] R.M. Gray. Toeplitz and circulant matrices: a review. *Foundations and Trends in Communications and Information Theory*, 2(5):155–239, 2006.

[24] P. Martin-Martin, F. Cruz-Roldan, and T. Saramäki. Optimized transmultiplexers for multirate systems. In *Proc. 2nd Intern. Symp. on Circuits and Systems, Kobe, Japan*, pages 1106–1109, 2005.

[25] R.K Soni, A. Jain, and R. Saxena. An optimized transmultiplexer using combinatorial window functions. *Signal Image Video Processes*, 5:389–397, 2011.

[26] Hamid Saeedi-Sourck, Yan Wu, Jan W.M. Bergmans, Saeed Sadri, and Behrouz Farhang-Boroujeny. Sensitivity analysis of offset qam multicarrier systems to residual carrier frequency and timing offsets. *Signal Processing*, 91(7):1604–1612, 2011.

[27] H. Lin, M. Gharba, and P. Siohan. Impact of time and carrier frequency offsets on the FBMC/OQAM modulation scheme. *Signal Processing Journal*, 2014.

[28] T.T. Nguyen, J.E. Salt, Ha.H. Nguyen, and B. Berscheid. Optimizing pulse shaping filter for DOCSIS systems. *IEEE Trans. Broadcasting*, 62(2):470–481, 2016.

[29] P. Biswas, S. Rathore, and M.R. Khan. A novel approach of various QAM with roll off factor variation using raised cosine filter and SRRC filter for analysis of BER and SNR. *Materials Today*, 2021.

[30] H.M Abdel-Atty, W.A. Raslan, and A.T. Khalil. Evaluation and analysis of FBMC-OQAM systems based on pulse shaping filters. *IEEE Access*, 8:55750–55772, 2020.

[31] Q. Bai and J.A. Nossek. On the effects of carrier frequency offset on cyclic prefix based OFDM and filter bank based multicarrier systems. In *Proc. IEEE 11th Intern. Workshop Signal Proc. Adv. Wireless Comm. (SPAWC), Marrakech, Morocco*, pages 1–5, 2010.

[32] P.R. Chevillat and G. Ungerboeck. An optimized transmultiplexer using combinatorial window functions. *IEEE Trans. Comm.*, COM-30(8):1909–1915, 1982.